H_2Open Journal

IWA PUBLISHING

H_2Open Journal Vol 7 No 2, 199 doi: 10.2166/h2oj.2024.110

Climate change and hydropower resilience in Nepal: an integrated modeling approach in the Madi River Basin

Pragya Pokharel and Ram Krishna Regmi *

Department of Civil Engineering, Institute of Engineering Pulchowk Campus, Tribhuvan University, Lalitpur, Nepal
*Corresponding author. E-mail: rkregmi@pcampus.edu.np

RKR, 0000-0002-8219-2127

ABSTRACT

Responding to Nepal's hydropower sector's vulnerability to climate change, this study investigates its impact on energy security, focusing on the Madi River Basin's river systems. This study conducted a rigorous analysis of the basin's historical and future hydroclimatic trends, using the linear scaling method to correct inherent biases in 13 GCMs, resulting in the selection of 6 BCMs with above-satisfactory performance. Future projections reveal an increase in annual precipitation with a higher increment in SSP585 by the end of the century, and a temperature rise ranging from 1.8 to 3.5 °C from the baseline in the far future under moderate- to high-emission scenarios. These hydroclimatic projections are then forced into the calibrated soil and water assessment tool (SWAT) model with very good performance (both R2 and NSE greater than 0.8). The streamflow projection demonstrates an overall increasing trend, marked by significant flow reduction in early months and pronounced monsoon peaks. The analysis of three distinct hydropower projects reveals unique challenges and opportunities, underscoring the heterogeneous nature of projects and the need for location-specific planning and strategic management. This study provides crucial insights for sustainable development in renewable energy, laying the foundation for future research and policy in similar hydroclimatic settings.

Key words: climate change, energy security, hydroclimatic trend, integrated modeling, linear scaling, SWAT model

HIGHLIGHTS

- Linear scaling is applicable for correcting bias in raw GCMs, enhancing climate projection reliability.
- CMIP6 projections reveal an increase in future precipitation and temperature in Nepal's Madi River Basin.
- SWAT model replicates the hydrologic response of the basin.
- Streamflow is projected to increase in the future, at annual and seasonal scales.
- Location-specific planning is needed in hydropower projects.

GRAPHICAL ABSTRACT

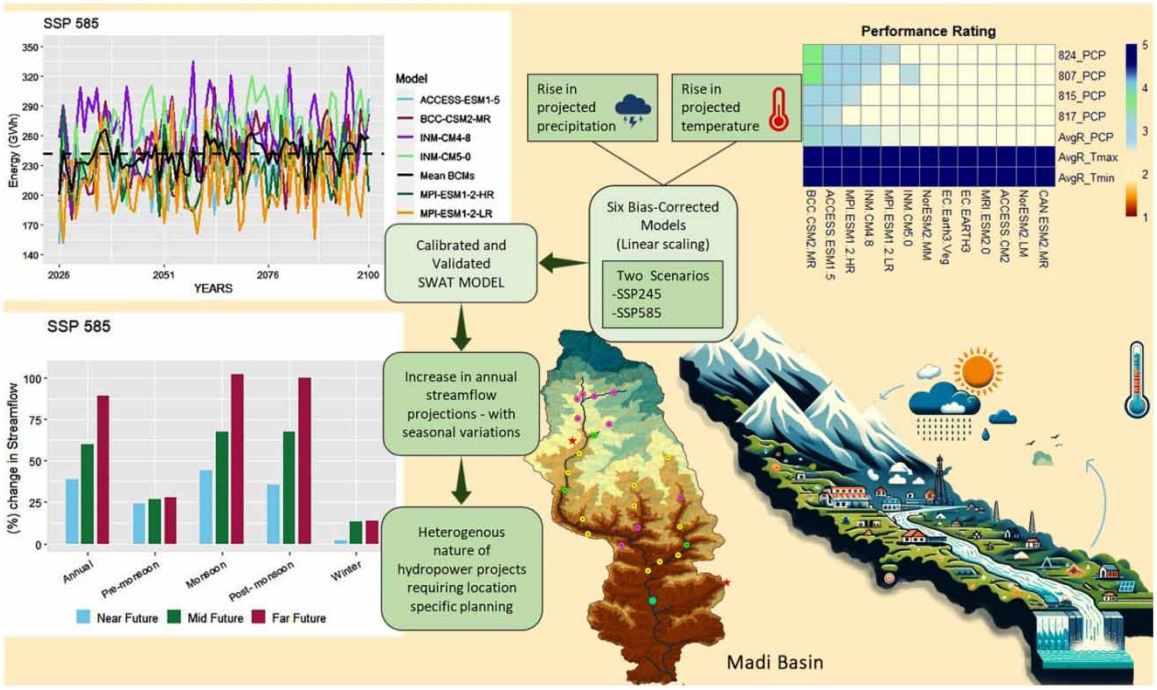

1. INTRODUCTION

Climate change represents one of the most pressing global challenges of our time, a fact affirmed by key international bodies such as the United Nations, the Intergovernmental Panel on Climate Change (IPCC), and the Paris Agreement. The United Nations' 2030 Agenda for Sustainable Development specifically emphasizes the urgent need for substantial action against climate change through Sustainable Development Goal 13, which calls for measures to combat climate change and its impacts (UNFCCC 2015). The IPCC verifies that climate change is real and primarily caused by human activities. Failure to significantly reduce greenhouse gas emissions could result in severe and irreversible changes (IPCC 2014).

In response to these concerns, the Paris Agreement, adopted in 2015, establishes a global framework to mitigate climate change by limiting global warming to well below 2 °C above pre-industrial levels, with an ideal target of 1.5 °C. It also encourages nations to establish and pursue their own nationally determined contributions (NDCs) to achieve these goals. As part of its NDC, Nepal has set an ambitious goal to increase its clean energy generation from a baseline of 1,400 to 15,000 MW by 2030. Nepal aims to meet 15% of its total energy demand through clean energy sources by the same year. This strategy demonstrates Nepal's firm commitment to aligning its national objectives with global climate change mitigation efforts (NDC 2020).

Hydropower plays a crucial role as a renewable energy source, boasting a global installed capacity of 1,360 GW in 2021 (IHA 2021). It provides environmental advantages, contributes to grid stability, and offers storage capacity (IPCC 2014; IRENA 2020; Baniya *et al.* 2023; Lamsal *et al.* 2023). However, the climate change is likely to affect hydropower, impacting energy security and grid reliability (Madani & Lund 2010; Hamududu & Killingtveit 2012; van Vliet *et al.* 2013). Hydropower in Nepal is highly vulnerable to climate-induced variations, including alterations in precipitation patterns and glacier melt dynamics, necessitating focused research (Xu *et al.* 2009; Bajracharya & Shrestha 2011; Hamududu & Killingtveit 2012; Shrestha *et al.* 2012; IPCC 2018). Despite the increasing integration of climate considerations into hydropower planning, there is still an emphasis on engineering resilience and risk management (Regmi *et al.* 2016; Dhakal *et al.* 2017; Poudel & Duex 2017). Within this broader context, the Madi River Basin emerges as a significant case study due to its hydropower potential and its status as a representative glacier-fed system in Nepal. Also, research and development is crucial for the sector's long-term sustainability and climate resilience (Koirala *et al.* 2016).

Nepal's hydrological landscape is distinctive, shaped by Himalayan snow and glacier melt (Xu *et al.* 2009; Bajracharya & Shrestha 2011). The Koshi, Narayani, and Karnali river basins, Nepal's three major basins,

hold a gross hydropower potential of 72,544 MW, constituting 94% of the country's total hydropower potential (WECS 2019). Presently, Nepal's hydroelectric production surpasses its peak demand, generating 1,964 MW against a demand of 1,748 MW (NEA 2022). However, to meet its NDC targets, a more diversified approach to renewable energy beyond hydropower is essential (WECS 2022).

Climate change is fundamentally altering global water cycles, impacting precipitation and evaporation patterns, as well as influencing streamflow and extreme weather events, especially in glacier-dependent areas (Hegerl *et al.* 2015; Van Lanen *et al.* 2016; Greve *et al.* 2018; IPCC 2019; Barzkar *et al.* 2022). These shifts have serious implications for water management, affecting water availability, quality, and timing (Haddeland *et al.* 2014). In Nepal, these effects are exacerbated by its unique Himalayan geography, leading to accelerated glacier retreat and altered hydrological characteristics of river basins (Bajracharya & Shrestha 2011; Huss & Hock 2018). Hydrological shifts in pattern, magnitude, and water availability in Nepal impact multiple sectors like hydropower, irrigation, water supply, and traditional livelihoods (Khadka *et al.* 2014; Ragettli *et al.* 2015; Dahal *et al.* 2016a, 2016b; Dhakal *et al.* 2019; Ojha *et al.* 2020). Recent studies reveal dual trends in precipitation, with a decline in extreme annual indices and an increase in season-specific dry days (Chhetri *et al.* 2021). In the Narayani basin, Bhattarai *et al.* (2018) show that rising temperatures influence both annual and seasonal streamflows, as well as the snowmelt contribution to river flow. This observation aligns with hydrological findings from the Madi River Basin, a sub-basin of Narayani, where researchers elucidated the marked seasonality of river flows, observing that the mean monthly flow during the summer monsoon period was up to 14 times higher than in the dry season, thereby shedding light on the significant role played by topographical and climatic conditions in shaping low-flow regimes (Khanal & Watanabe 2017). Furthermore, a study by Burgan (2022) illustrates the utility of artificial neural networks (ANNs), such as feed-forward back propagation (FFBP), generalized regression neural networks (GRNN), and radial basis function (RBF) neural networks for enhancing daily streamflow predictions in the Kocasu River, Turkey. This advancement underscores the potential of similar predictive technologies to improve the accuracy of streamflow forecasts in Nepal's complex hydrological settings.

Understanding the vulnerabilities of regions like the Madi River Basin necessitates the utilization of advanced climate and hydrological models. Climate models, particularly those from the climate model intercomparison project (CMIP), serve as foundational tools for understanding hydrological responses under variant climatic conditions (Milly *et al.* 2008). The most recent phase, CMIP6, enriches these evaluations by accounting for anthropogenic influences, notably greenhouse gas emissions (Eyring *et al.* 2016). By integrating shared socioeconomic pathways (SSPs), CMIP6 facilitates intricate hydrological analyses that are especially vital for localized contexts, such as Nepal (O'Neill *et al.* 2016; Pandey *et al.* 2018; Reidmiller *et al.* 2018). Specifically, this study integrates two representative SSPs – SSP245 and SSP585 for comprehensive insights into moderate and high-emission scenarios, respectively. Downscaling techniques are employed to enhance the granularity of these models, thereby making them aptly suited for localized studies in areas such as Nepal (Teutschbein & Seibert 2012; Mishra *et al.* 2020).

Hydrological modeling, essential for managing water resources in mountainous terrains, has benefited from methodological advancements tailored to complex environments like the Himalayas (Bajracharya & Shrestha 2011; Immerzeel *et al.* 2020). Among various methods, the soil and water assessment tool (SWAT) stands out for its flexibility in representing intricate landscapes and hydrological conditions, including its applicability for climate change impact assessments (Arnold *et al.* 1998; Gassman *et al.* 2007; Zhang *et al.* 2009). Various case studies in Nepalese Himalayan Basins substantiate the capability of capturing the complexities of these regions (Shrestha *et al.* 2013; Babel *et al.* 2014; Ragettli *et al.* 2015; Bhattarai *et al.* 2016; Dahal *et al.* 2016a, 2016b; Bista *et al.* 2021).

Nepal's hydropower infrastructure, predominantly reliant on glacier- and snow-fed rivers, is highly vulnerable to climate change (Xu *et al.* 2009; Shrestha *et al.* 2012). Despite hydropower's centrality to Nepal's energy portfolio, studies at the river basin level addressing climate impact are limited, creating a knowledge gap (Dhakal *et al.* 2019; Shrestha *et al.* 2019). While studies have begun to investigate the vulnerabilities of Nepal's hydropower sector to climate change, they often focus on larger basins or issues like glacier melt and monsoon patterns (Shrestha *et al.* 2013; Bhattarai *et al.* 2016). The urgency of addressing climate impacts on hydropower generation at the sub-basin level remains underemphasized (Shrestha *et al.* 2019). The Madi River Basin, a tributary of the larger Narayani basin, exemplifies this research gap. Although prior work has identified 72 potential hydropower sites along the Madi's tributaries (Pokharel *et al.* 2020), comprehensive studies assessing the climate change impacts on hydropower generation within this specific basin are markedly absent.

In response to identified research gaps and the pressing need for focused inquiry, this study is primarily aimed at investigating the effects of climate change on hydrological characteristics and hydropower projects in the Madi

River Basin. The study endeavors to achieve three main objectives: (1) assess and analyze the baseline hydroclimatic trends in the region; (2) quantify the impacts of climate change on streamflow patterns; and (3) examine how these climatic changes influence hydroelectric energy production concerning established baseline energy figures. By pursuing these objectives, the study seeks to enhance understanding of the Madi Basin's resilience to evolving climatic conditions, thereby contributing to Nepal's strategies for climate-resilient hydropower development.

2. MATERIALS AND METHODS

This framework systematically investigates the impact of climate change on hydropower generation. The structured methodology integrates hydrological modeling, climate projections, energy computation, and impact assessment into a comprehensive framework as shown in Figure 1.

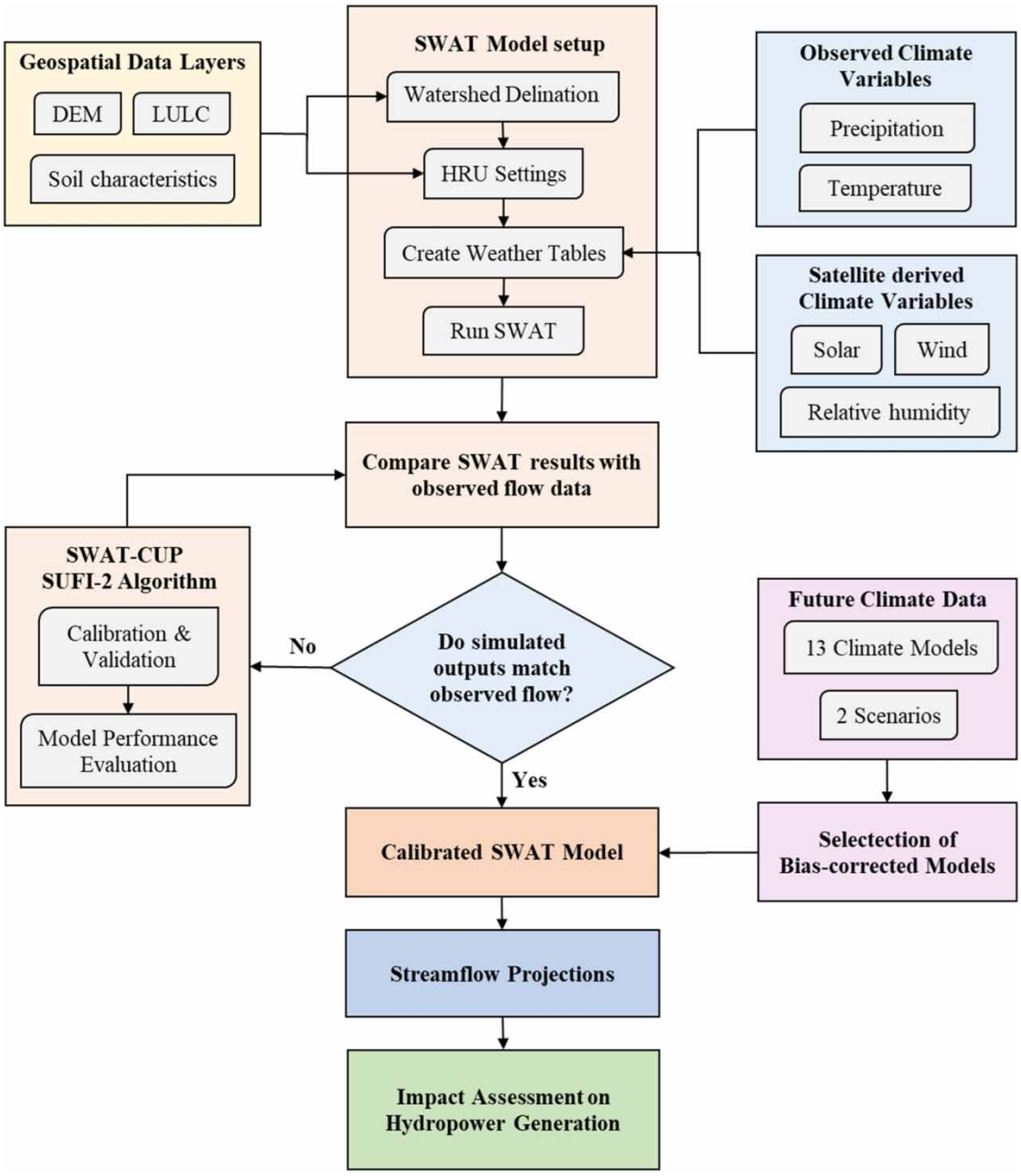

Figure 1 | The methodological framework for analyzing the impact of climate change on water resources and hydropower generation.

2.1. Study area

The Madi watershed, located in the central region of Nepal within Province-4, occupies a drainage area of approximately 1,122 km², ranging in altitude from 7,936 m to a minimum of 305 m, covering a north–south distance of about 68 km (Figure 2). The watershed's outlet is at the Byas cave of Damauli, positioned at 27°58′12.72″N latitude and 84°15′59.40″E longitude. The annual precipitation within the Madi watershed varies significantly, from a mean of 1,684 mm at Damauli in the southern region to 3,784 mm at Sikles in the north. Approximately 74–80% of the total precipitation occurs during the four summer monsoon months, from June to September.

The Madi River, also known as Madikhola, originates from the Annapurna II glacier and is supplemented by other features like the Kahphuche Lake. The lake was formed as a result of the melting of ice sheets that pooled in a lower area (Koirala *et al.* 2017). Uniquely, the lake is formed at a relatively low altitude for glacial lakes in the Nepal Himalayas. By 2020, the lake's area was estimated to be 0.12 ± 0.015 km^2, with a volume of 1.42×10^6 m^3 according to bathymetric data (Kandel *et al.* 2023). The Madi River has a total of 14 tributaries, the largest is the Midim, and the others include Rudi, Madkyu, Kyaduso, Nyache, Idi, and Madame supporting various capacities of hydropower projects. The remaining tributaries – Paste, Birdi, Khalte, Pisti, Risti, Sange, and Kalesti – are located at the lower elevations of the watershed.

At present, there are 23 hydropower projects either at the operation, generation, or survey license phase in the Madi basin. Taken together, the potential power generation for the Madi River Basin stands at 377.37 MW, a notable output for a basin of its size. To address the impacts of climate change and ensure the representation of diverse geographical areas, projects have been selected to optimally represent the flow conditions of the tributaries. The three selected hydro projects are presented in Table 1.

2.2. Data acquisition and processing

This study required the acquisition and preprocessing of various primary as well as secondary spatial-temporal datasets. The digital elevation model (DEM) data used in this study were obtained from the Shuttle Radar Topography Mission (SRTM). The chosen SRTM DEM had a spatial resolution of 30 m × 30 m. Land use land cover

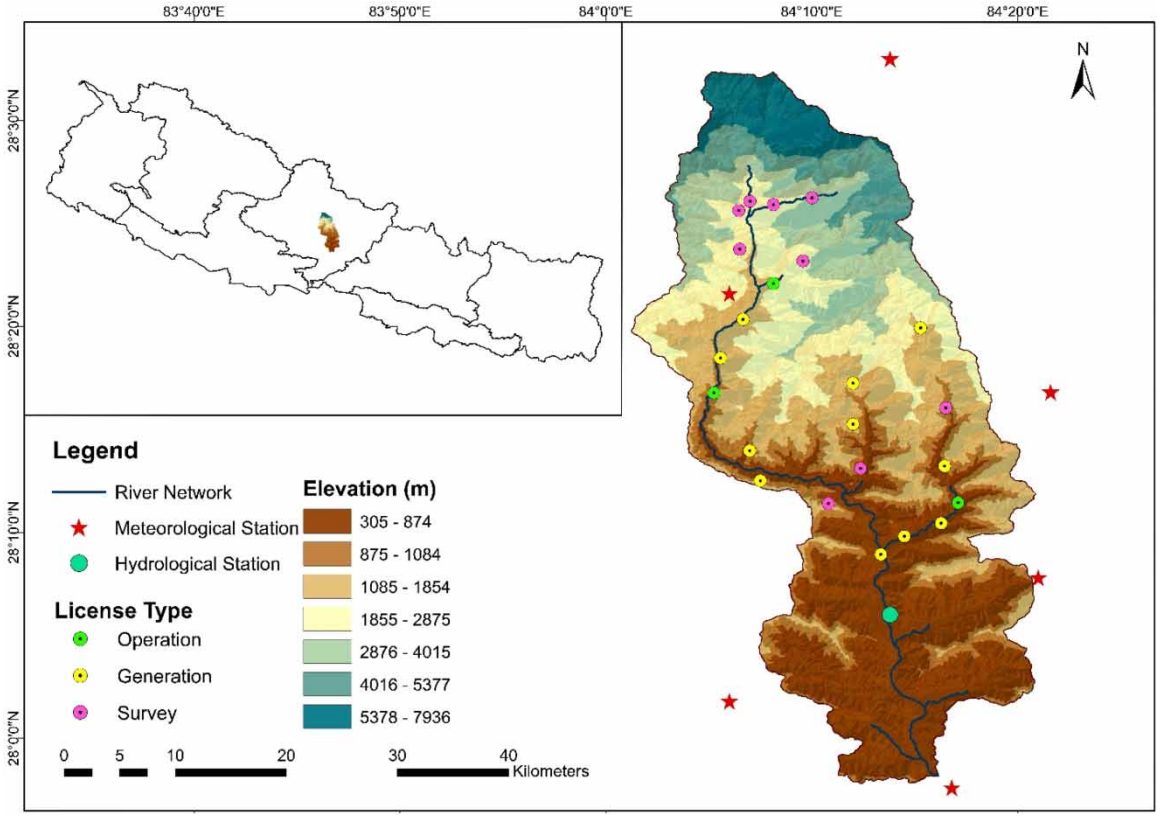

Figure 2 | Study area map showing hydrometeorological stations and hydropower projects in the Madi River Basin.

Table 1 | Characteristics of hydropower projects selected for study

Hydropower project	Location	Capacity (MW)	Lat. (°N)	Long. (°E)	License type	Q_d (m³/s)	C. area (km²)	Net head (m)
Madme Khola HPP	Upper Tributary	24	28.43	84.14	Survey	5.18	48.7	536.02
Super Madi HPP	Madi River	44	28.34	84.11	Generation	18	284.1	295
Midim Khola HPP	Lower Tributary	3	28.19	84.29	Operation	7.30	136.5	48.69

(LULC) data were obtained from the regional database system (RDS) of ICIMOD for the year 2017, featuring 11 land use classes with a 30 m × 30 m resolution (FRTC & ICIMOD 2021). Seven land use classes were identified within the study area with forest being dominant, occupying approximately 66.89% of the total area. Agriculture is the second most abundant land use, covering 15.15% of the watershed, while Glacier/Snow covers 7.25%. The soil data for this study were obtained from the Soil and Terrain Database (SOTER) for Nepal, developed by the International Soil Resources and Information Center (ISRIC) with a spatial resolution of 1:1 million (Dijkshoorn & Huting 2009). Within the study area, six soil classes were identified, with Eutric Cambisoils (CMe) as the predominant class, encompassing 44.36% of the basin area (Figure 3).

The historical hydroclimatic data required for this study include daily precipitation, minimum and maximum temperature, and observed streamflow data, which were sourced from the Department of Hydrology and Meteorology (DHM), Government of Nepal. In the vicinity of the Madi River Basin, six climatic stations and one hydrologic station were strategically selected to provide relevant and overall coverage (Figure 2). The statistical measures for annual hydroclimatic variables at hydrometeorological stations (Table 3), encompassing descriptive statistics, measures of variability, shape characteristics, confidence intervals, and distribution properties, are detailed in Supplementary Table S1.

Future climate projection refers to the use of scientific methods and computational models that enable the prediction of future climatic conditions over various time scales, such as decades or centuries (IPCC 2013). Bias in precipitation and temperature data from global climate models (GCM) often arises from the models' coarse resolution or the way they are parameterized (Mishra *et al.* 2020). To address this, Mishra *et al.* (2020) utilized 13 CMIP6-GCM models with spatial resolutions ranging from 0.7° to 0.2° under r1i1p1f1 initial conditions for both historical (1850–2014) and future (2015–2100) climate under four SSPs (SSP126, SSP245, SSP370, and SSP585). Using both dynamic and statistical approaches, climate data were produced for six South Asian countries, including Nepal. Thus, downscaled and bias-corrected daily climate data to a spatial resolution of approximately 0.25° (around 28 km at the equator) were used in this study (available at https://doi.org/10.5281/zenodo.3987736).

Furthermore, two scenarios, SSP245 and SSP585, were selected for this study, so even with less computation, we could explore a wide range of potential future climate conditions, i.e., from a moderate pathway where some mitigation efforts are made, representing a 'balanced case' scenario (SSP245) to a more extreme pathway with high emissions and little mitigation are made, typically representing 'worst case' scenario (SSP585) (Riahi *et al.* 2017). The GCM models used in this study for performance evaluation are listed in Table 2.

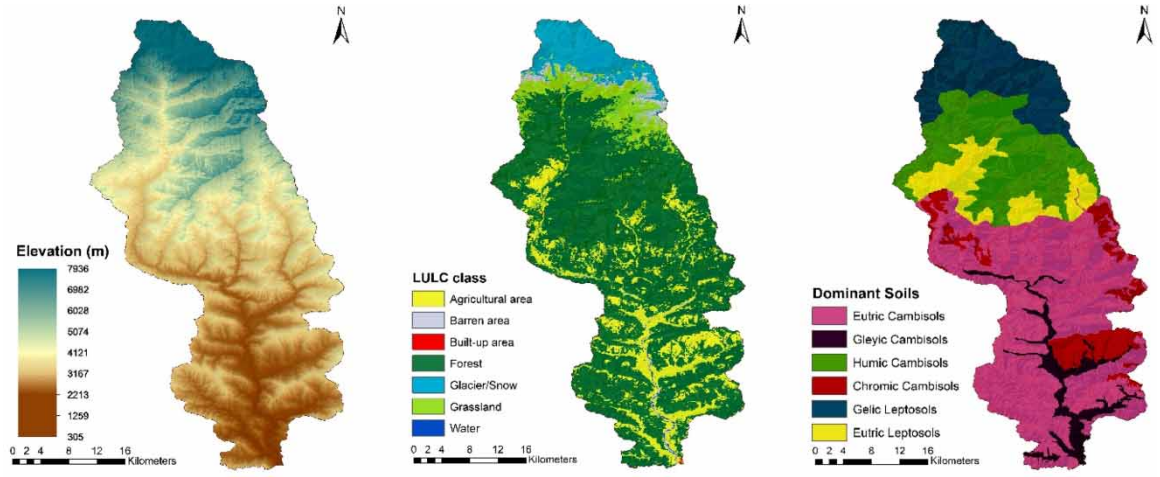

Figure 3 | DEM, land use map, and soil map.

Table 2 | The climate models of CMIP6 used in this study

Model name	Modeling center/group	Country
BCC-CSM2-MR	Beijing Climate Center	China
ACCESS-ESMI-5	Commonwealth Scientific and Industrial Research Organization	Australia
MPI-ESMI-2-HR	Max Plank Institute for Meteorology	Germany
INM-CM4-8	Institute for Numerical Mathematics	Russia
MPI-ESM-2-LR	Max Plank Institute for Meteorology	Germany
INM-CM5-0	Institute for Numerical Mathematics	Russia
NorESM2-MM	Norwegian Climate Center	Norway
EC-Earth3-Veg	EC-Earth Consortium	Europe
EC-Earth3	EC-Earth Consortium	Europe
MRI-ESM2-0	Meteorological Research Institute	Japan
ACCESS-CM2	Commonwealth Scientific and Industrial Research Organization -Australian Research Council Centre of Excellence for Climate System Science (CSIRO-ARCCSS)	Australia
NorESM2-LM	Norwegian Climate Center	Norway
CanESM5	Canadian Center for Climate Modelling and Analysis	Canada

2.3. Trend analysis on historical observation

Trend analysis on hydroclimatic variables is an indispensable technique in understanding the dynamic nature of climatic processes over time. In this research, the trend analysis is performed at chosen hydrometeorological stations listed in Table 3, focusing on available time series data at multiple temporal scales, i.e., seasonal and annual. The analysis is performed using two methods: Mann–Kendall test and Sen's slope test. The Mann–Kendall test is a non-parametric statistical method used to identify trends in time series data (Mann 1945; Kendall 1975). Following the trend detection by the Mann–Kendall test, Sen's slope test is employed to quantify the slope of the trend (Sen 1968).

2.4. Hydrological modeling

SWAT is a physically based semi-distributed, continuous-time model used to generate streamflow for large, complex watersheds with varying soils, land use, and weather conditions, essential for understanding the selected region's hydrological behavior (Arnold *et al.* 1998). The selection of SWAT is guided by its proven capabilities in representing complex hydrological processes with a considerable degree of accuracy. The model's functioning is governed by the water balance equation (Equation (1)) representing the conservation of mass in the soil profile, essential in predicting the hydrological response of the watershed (Neitsch *et al.* 2011).

$$\mathrm{SW}_t = \mathrm{SW}_0 + \sum_{i=1}^{t} (R_{\mathrm{day}} - Q_{\mathrm{surf}} - E_{\mathrm{a}} - W_{\mathrm{seep}} - Q_{\mathrm{gw}}) \quad (1)$$

Table 3 | Hydrometeorological stations used for trend analysis

Data	Station		Data period
	Index No.	Name	
Precipitation	824	Siklesh	1985–2019
	807	Kunchha	
	817	Damauli	
Temperature	815	Khairenitar	1980–2019
Streamflow	438	Sisha Ghat	1985–2015

where SW_t and SW_0 are the final and initial soil water content (mm), t is the time (days), R_{day} is daily precipitation (mm), Q_{surf} is the daily surface runoff (mm), E_a is the daily evapotranspiration (mm), W_{seep} is the daily percolation and bypass flow (mm), and Q_{gw} is the daily return flow/base flow (mm).

Surface runoff was estimated using the soil conservation service curve number (SCS Curve number) method:

$$Q_{surf} = \frac{(R_{day} - I_a)^2}{(P_{day} - I_a - S)} \tag{2}$$

where I_a is the initial abstraction which includes surface storage, interception, and infiltration prior to runoff and S is the retention parameter (mm).

The retention parameter is defined by:

$$S = 25.4 \left(\frac{1,000}{CN} - 10 \right) \tag{3}$$

where CN is the curve number for the day varying from 0 to 100 depending on soil permeability, land use, and the antecedent soil water condition.

2.4.1. Model setup

The process of setting up the SWAT model in this study begins with the preprocessing and loading of the DEM into the model (Neitsch *et al.* 2011). Watershed delineation was then performed, with a drainage threshold area (DTA) set at 500 ha, a critical parameter that determines the stream network within the watershed, defining the size and configuration of the sub-basins (Arnold *et al.* 2012). Monitoring points were manually added, incorporating a hydrological station as an outlet and carefully selecting the final outlet at Byas Cave, and then the watershed was discretized into 12 sub-basins. Subsequently, five slope classes were defined as follows: 0–5%, 5–15%, 15–30%, 30–50%, and above 50%. The threshold area for land, soil, and slope class was set at 10%, ensuring that only major features were represented in the model (Arnold *et al.* 2012). The discretization continued with the creation of 130 HRUs, each representing a unique combination of land use, soil type, and slope class within a sub-basin. Daily weather inputs, such as precipitation, solar radiation, relative humidity, wind, and maximum and minimum temperature data, were imported into SWAT through the weather input station, and any missing data were generated using the model's inbuilt stochastic weather generator. For surface runoff estimation, the SCS curve number method was applied, and no point sources were defined in this model setup. Lastly, the Penman–Monteith method was employed for potential evapotranspiration (PET) calculations, favored for its comprehensiveness and ability to account for various atmospheric and surface conditions (Allen *et al.* 1998).

2.4.2. Sensitivity analysis and calibration approach

The sequential uncertainty fitting (SUFI-2) algorithm in SWAT calibration and uncertainty programs (SWAT-CUP) was employed to perform sensitivity analysis, calibration, and validation. Specifically, the model was calibrated for one hydrological station, Sisha Ghat, over 12 years from 2004 to 2015, with the first 4 years serving as a warm-up phase. The model was subsequently calibrated using daily discharge data for the next 5 years, 2008–2012, and validated for the following 3 years, 2013–2015. Global sensitivity analysis was adopted in this study. The parameters were methodically selected through a two-stage process: first, by analyzing the behavior of the initial model through a single simulation and performing parameter regionalization as suggested by Abbaspour *et al.* (2015), and second, by drawing from previous studies conducted on Gandaki Basin and in other Himalayan watersheds in Nepal (Devkota & Gyawali 2015; Pandey *et al.* 2020; Pokharel *et al.* 2020). The goodness of fit was quantified by analyzing the 95% prediction uncertainty (95PPU) band. Key metrics in this assessment were the P-factor and R-factor, with optimal values being a P-factor approaching 1 and an R-factor approaching 0, with criteria set for good fit for flow data at $P > 0.7$ and $R < 1.2$ (Abbaspour *et al.* 2017). This robust methodology ensures the reliability and precision of the hydrological modeling before the model performance indicator.

2.4.3. Performance evaluation criteria

Three primary error metrics were used for this evaluation: Nash–Sutcliffe Efficiency (NSE), coefficient of determination (R^2), and percentage bias (PBIAS). NSE is a significant metric, representing how well the variance in observed data is represented by the model, with a value of 1 indicating perfect estimation and thus signifying an

accurate model (Krause *et al.* 2005). On the other hand, the coefficient of determination, R^2, informs the correlation between observed and simulated values. The PBIAS is another vital parameter; a positive value represents an overestimation while a negative value indicates underestimation. The low absolute value of PBIAS further signifies the superior performance of the model. Criteria for judging the efficiency of the model include R^2 values greater than 0.70, NSE values greater than 0.75, and the PBIAS value less than $\pm 10\%$, solidifying the model's validity and reliability. According to Moriasi *et al.* (2007), these parameters are indispensable for understanding the accuracy of hydrological models.

2.5. Future climate projection

For this study, precipitation and temperature projections were analyzed up until the end of the century (2026–2100), focusing on the potential impacts on streamflow. The baseline historical data for comparison purposes were taken from the years 1995 to 2019. Bias correction is a statistical technique that can be used independently of downscaling and is essential to make the model outputs more accurate and useful for impact assessment (Maraun *et al.* 2010). Due to the elongated characteristics of the watershed, despite its small area, it contained one gridded station near the DHM station Siklesh (824) and three in the vicinity of Khairenitar (815), Kunchha (807), and Damauli (817). Thus, data retrieved from Mishra *et al.* (2020) were bias-corrected using the nearest station's climate data. The bias correction was carried out using the linear scaling method, a simple yet effective method. This method perfectly adjusts the monthly mean of raw GCM output to the observed value without excessively altering the underlying distribution of values, ensuring the natural variability in the climate (Maraun *et al.* 2010; Teutschbein & Seibert 2012). Compared to other complex bias correction techniques, the linear scaling method is both simple and effective (Shrestha *et al.* 2017).

The performance analysis of GCM and bias-corrected models (BCM) is an imperative step in enhancing the reliability and accuracy of climate projections. It ensures that the corrected models retain the essential physical processes and spatial patterns captured by the raw GCM (Teutschbein & Seibert 2012). In this study, the performance of climate data was evaluated for both raw GCM and BCM against the baseline monthly observed data at four selected DHM stations (824, 807, 815, and 817). Utilizing three key performance metrics – Nash Sutcliffe efficiency (NSE), ratio of the root mean square error to the standard deviation of observed data (RSR), and PBIAS – the climate data were analyzed, and individual performance metrics were computed for all 13 raw GCMs and BCMs. The ranking done based on the average of combined performance ratings as shown in Table 4 (Timilsina *et al.* 2021) enabled the subsequent selection of the top six BCMs listed in Table 2. This study adopts a similar approach to Baniya (2022), utilizing heat map representations to effectively convey both individual metric values and their collective ratings for the selected stations.

2.6. Hydro-energy generation

The fundamental equation used for calculating the hydro-energy generation is given by the following equation,

$$P = \eta \cdot \rho \cdot g \cdot Q \cdot H \tag{4}$$

where P is the power generated, η is the efficiency of the turbine, ρ is the density of water, g is the gravitational acceleration, Q is the flow rate, and H is the head or height of the water above the turbine. In this study, the simulated future streamflow data ensuring the design discharge was deployed in the power equation. Furthermore, the net head and efficiency of respective hydropower projects were incorporated within the calculations ensuring the

Table 4 | Performance rating criteria

Model evaluation	NSE	RSR	PBIAS	Rating
Very Good	$0.75 < \text{NSE} \leq 1.00$	$0.00 < \text{RSR} \leq 0.50$	$\text{PBIAS} \leq \pm 10\%$	5
Good	$0.65 < \text{NSE} \leq 0.75$	$0.50 < \text{RSR} \leq 0.70$	$\pm 10\% < \text{PBIAS} \leq \pm 15\%$	4
Satisfactory	$0.50 < \text{NSE} \leq 0.65$	$0.60 \leq \text{RSR} \leq 0.70$	$\pm 15 < \%\ \text{PBIAS} \leq \pm 25\%$	3
Unsatisfactory	$0.40 < \text{NSE} \leq 0.55$	$0.70 \leq \text{RSR} \leq 0.50$	$\pm 25\% < \text{PBIAS} \geq \pm\ 35\%$	2
Poor	$\text{NSE} \leq 0.4$	$0.80 < \text{RSR}$	$\pm 35\% < \text{PBIAS}$	1

potential variations in flow as well as design constraints of projects. Finally, the energy computation was done by integrating the power equation over time, every month.

2.7. Climate change impact assessment

The model performance of the SWAT model was evaluated for calibration and validation purposes considering streamflow observations from 2004 to 2015. Subsequently, this model was employed for the extended period from 1990 to 2019 with the first 5 years as a warmup, to simulate baseline streamflow. This well-calibrated model was then forced with future climate data spanning from 2026 to 2100, to generate continuous streamflow projections. By comparing these projections with the established baseline, the possible climate change implications on the hydrological characteristics are quantified at annual and seasonal scales. Focusing on three selected hydropower projects, the climate change impact on energy generation was calculated. This analysis was performed on annual and monthly scales at three distinct 25-year intervals: Near Future (2026–2050), Mid Future (2051–2075), and Far Future (2076–2100) scenarios, termed as NF, MF, and FF, respectively.

3. RESULTS AND DISCUSSION

3.1. Hydroclimatic trend

The annual trend of streamflow at Sisha Ghat shows a significant decrease at a rate of −0.4487 cumec/year ($p = 0.01574$), indicative of a substantial reduction in flow. This decline is most prominent during the monsoon season with a rate of −1.3066 cumec/year ($p = 0.0086$), while the pre-monsoon trend is negligible. Post-monsoon and winter seasons present slightly positive trends, though they are not statistically significant. The temperature at Khairenitar demonstrates a consistent and significantly increasing trend across all seasons, with the annual rate at 0.0288 °C/year ($p = 0.0001$). The precipitation trend of the upper watershed reveals a negligible annual trend, suggesting a stable precipitation pattern in this area. The annual trend in lower watershed indicates a significantly decreasing rate of −16.84 mm/year ($p = 0.00412$), particularly notable in the monsoon season at a rate of −10.49 mm/year ($p = 0.021$). The precipitation trend of the upper watershed reveals a negligible annual trend, suggesting a stable precipitation pattern in this area. The annual trend in lower watershed indicates a significantly decreasing rate of −16.84 mm/year ($p = 0.00412$), particularly notable in the monsoon season at a rate of −10.49 mm/year ($p = 0.021$).

The summary of trend analysis (computed at 5% significance level) is presented in Figure 4 (Supplementary Table S2). The trends reveal significant variations in hydroclimatic factors across different portions of the watershed.

The significant decrease in annual and monsoon streamflow may be due to altered precipitation patterns, land use, increased water consumption, or groundwater recharge. The significant temperature rise could be indicative of broader climatic shifts or localized anthropogenic influences such as urbanization. The contrasting trends in precipitation between upper and lower watersheds possibly reflect spatial weather variations or topographical influences on rain distribution.

3.2. SWAT model parameter sensitivity and performance evaluation

The performance evaluation of the SWAT model is crucial for assessing its ability to simulate real field scenarios. Out of 21 chosen parameters, 15 are identified as the most sensitive. Since the trend analysis reveals topographical effects, the calibration of the SWAT model at the Sisha Ghat station is conducted first, with specific attention to elevation parameters such as temperature lapse rate (TLAPS) and precipitation lapse rate (PLAPS). Among these, the PLAPS parameter emerges as the most sensitive, with a positive value that indicates an increase in precipitation with increasing elevation. Previous studies (Pandey *et al.* 2020; Baniya 2022) in Himalayan catchment have found similar sensitivity of these parameters due to the orographic effect. Then among snow parameters, snowfall temperature (SFTMP) is identified as the most sensitive.

Further sensitivity analysis highlights that surface release and groundwater movement exert substantial influence on the basin. Geomorphological factors, OV_N (Manning's n value for overland flow) and SLSUBBSN (average slope length) are found to be highly sensitive. The groundwater-sensitive parameter GW_DELAY, controlling groundwater behavior, and the saturated hydraulic conductivity SOL_K (), affecting the basin's surface runoff, have a dominant effect as well. The remaining parameters are ranked and tabulated according to their sensitivity from 1 to 15, with 1 being the most sensitive (Table 5).

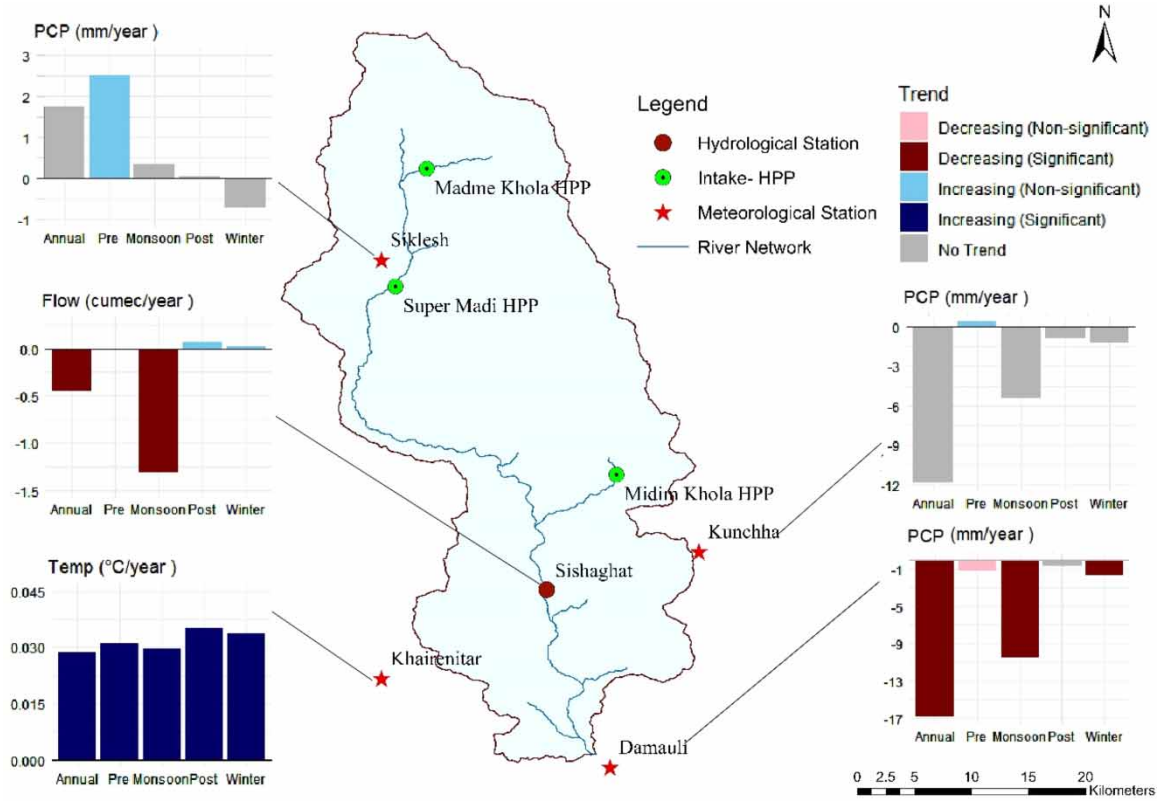

Figure 4 | Seasonal and annual trends of hydroclimatic variables based on a 95% confidence level. HPP, hydropower project; PCP, precipitation; Temp, temperature.

Table 5 | Parameters' ranking based on their sensitives along with their fitted values

S. N	Parameters	Fitted value	Min value	Max value
1	r__OV_N.hru	139.12	1.00	150.00
2	v__GW_DELAY.gw	23.84	12.70	37.74
3	v__PLAPS.sub	97.41	33.45	106.55
4	v__SFTMP.bsn	2.00	−4.46	2.06
5	r__SOL_K().sol	−0.60	−1.18	−0.48
6	r__SLSUBBSN.hru	14.31	2.00	15.00
7	r__SURLAG.bsn	1.54	−6.19	13.39
8	v__SOL_AWC().sol	0.73	0.65	0.78
9	r__CN2.mgt	−0.18	−0.30	−0.10
10	v__LAT_TTIME.hru	6.86	−32.21	45.47
11	v__ESCO.hru	1.00	0.99	1.01
12	v__GWQMN.gw	192.29	156.41	266.14
13	v__CH_N2.rte	0.21	0.17	0.25
14	r__HRU_SLP.hru	0.24	0.10	0.27
15	v__REVAPMN.gw	2,600.75	2,000.00	2,908.86

The evaluation of the hydrological model for both calibration (2008–2012) and validation (2013–2015) yielded results that fall within the 'Very Good' category (Moriasi *et al.* 2007), with $R^2 > 0.7$ and NSE > 0.75 (Table 6). These results indicate a strong correlation between observed and simulated values, emphasizing the model's ability to reproduce the variance in observed data. The simulation of daily hydrographs for the calibration and validation periods is shown in Figure 5.

Table 6 | Performance metrics of daily streamflow during the calibration and validation period

Process	Year	R^2	NSE	PBIAS (%)
Calibration	2008–2012	0.80	0.84	10.6
Validation	2013–2015	0.83	0.82	9.9

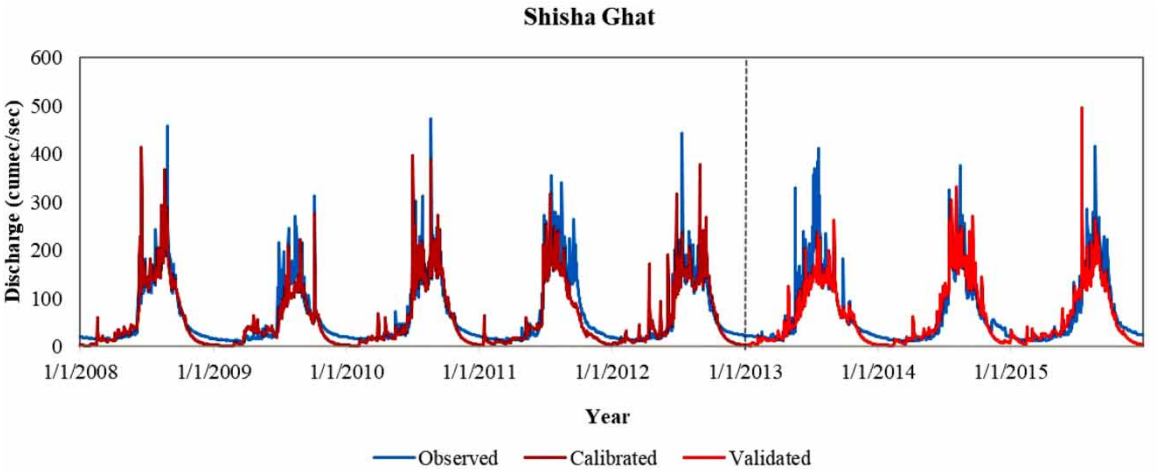

Figure 5 | Observed and simulated daily discharge hydrograph during calibration (2008–2012) and validation (2013–2015) periods at Sisha Ghat hydrological station.

3.3. Climate model performance

Evaluating GCMs against observed data is vital in identifying inherent biases and guiding subsequent refinements to enhance model accuracy. The performance evaluation of GCM and BCM is carried out on a monthly scale at four climate stations: Siklesh (824), Kunchha (807), Khairenitar (815), and Damauli (817). Individual statistical parameter performance NSE, RSR, and PBIAS along with their collective performance are computed based on Table 4.

3.3.1. Comparison of raw GCM with observed DHM

The performance evaluation of GCM indicates a pronounced need for bias correction (Figure 6). While all GCMs successfully capture the variation of temperature data, yielding good and very good performance ratings, the results are more complex for precipitation. Specifically, individual performance levels for precipitation reveal a negative NSE at the Damauli station and high RSR values at both the Damauli and Siklesh stations. Furthermore, the stations Siklesh and Kunchha display an overestimation of monthly data. The overall performance for precipitation is noticeably poorer in correlation compared to temperature. Among 13 models, CanESM5 exhibits an unacceptable performance in both NSE and RSR. Thus, these findings emphasize the critical role of a rigorous bias correction process to enhance the usability and reliability of GCM outputs in climate impact assessments.

3.3.2. Comparison of BCM with observed DHM

Given the identified biases in the raw GCM results, the linear scaling method is used to adjust the monthly mean outputs to align with observed values (Figure 7). For temperature, all metrics demonstrate very good performance, with a rating of 5.

Particularly notable is the PBIAS metrics' correction of precipitation, resulting in a very good performance, also rated as 5. The NSE values for most models have been uplifted from poorer to satisfactory levels, while only a few models display satisfactory results in RSR.

A collective improvement in overall ratings has been observed, with BCC-CSM2-MR at the top of the rank and CanESM5 at the bottom. Out of 13 BCMs, the top six models, namely BCC-CSM2-MR, ACCESS-ESM1-5, MPI-ESM1-2-HR, INM-CNM4-8, MPI-ESM1-2-LR, and INM-CM5-0, have been selected for future climate projection,

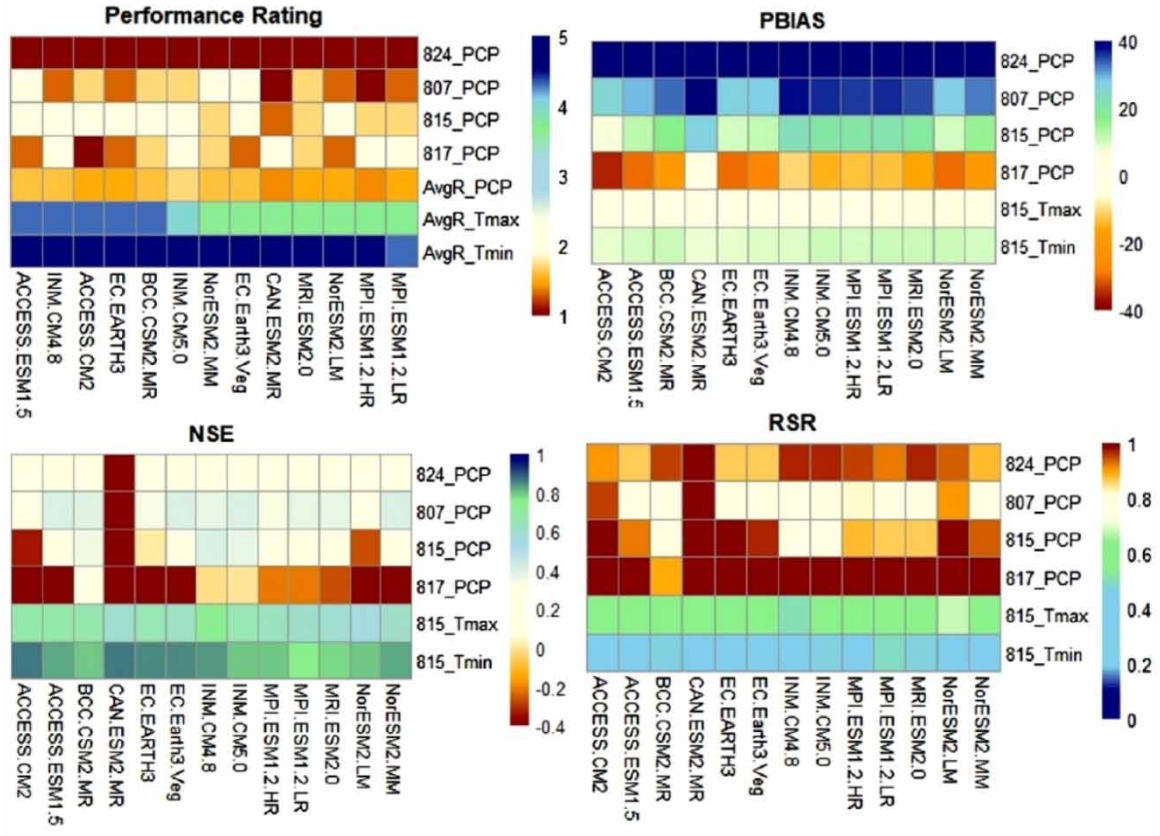

Figure 6 | Performance ratings of raw GCMs. In the top-left sub-plot, ranking 1–13 follows the order while moving from left to right.

as they collectively achieve above-satisfactory results for precipitation. Ultimately, the application of linear scaling has further enhanced these models' accuracy and reliability.

3.4. Climate and streamflow projections

Climate change projection utilizes previously selected six BCMs at two emission levels, SSP245 and SSP585 at four stations, Siklesh (824), Kunchha (807), Khairenitar (815), and Damauli (817). The projected timeframe of 2026–2100 has been divided into three intervals, the near future (2026–2050), the mid future (2051–2075), and the far future (2076–2100). Within these intervals, the projections have been interpreted graphically.

3.4.1. Projected precipitation

The models representing the wetter and drier climate are ACCESS-ESM1-5 and MPI-ESM1-2-LR, respectively. The projected average annual precipitation from BCM projections at the watershed level is illustrated in Supplementary Figure S1. A broad observation reveals a general trend of increasing precipitation over the years, with occasional dips. The increasing trend is more pronounced in SSP585 as precipitation spikes in FF. Compared to the historical baseline level of 2,240.13 mm, precipitation is projected to increase in the FF period by approximately 1,716.95 mm, or 76.64%, under SSP245, and by approximately 2,424.71 mm, or 108.24%, under SSP585. Furthermore, the average annual and seasonal percentage change illustrated in Figure 8 (Supplementary Table S3) provides insights into the temporal fluctuations and seasonal dynamics of the watershed. The SSP245 scenario exhibits a general increase across all timeframes and seasons. The highest growth is evident in the post-monsoon season, especially in both NF and FF, with an increment of 80.4 and 82.73%, respectively. In contrast, SSP585 illustrates a more pronounced upward trend, particularly in the FF across all seasons. This is most noticeable in the monsoon and post-monsoon seasons, reaching as high as 119.39 and 137.42%, respectively, in the FF.

For both scenarios, the winter season undergoes relatively smaller increments compared to the other seasons. Given the projected substantial increases in precipitation, particularly under the SSP585 scenario, there is a heightened risk of extreme hydrological events that could exacerbate risks associated with exceptionally high

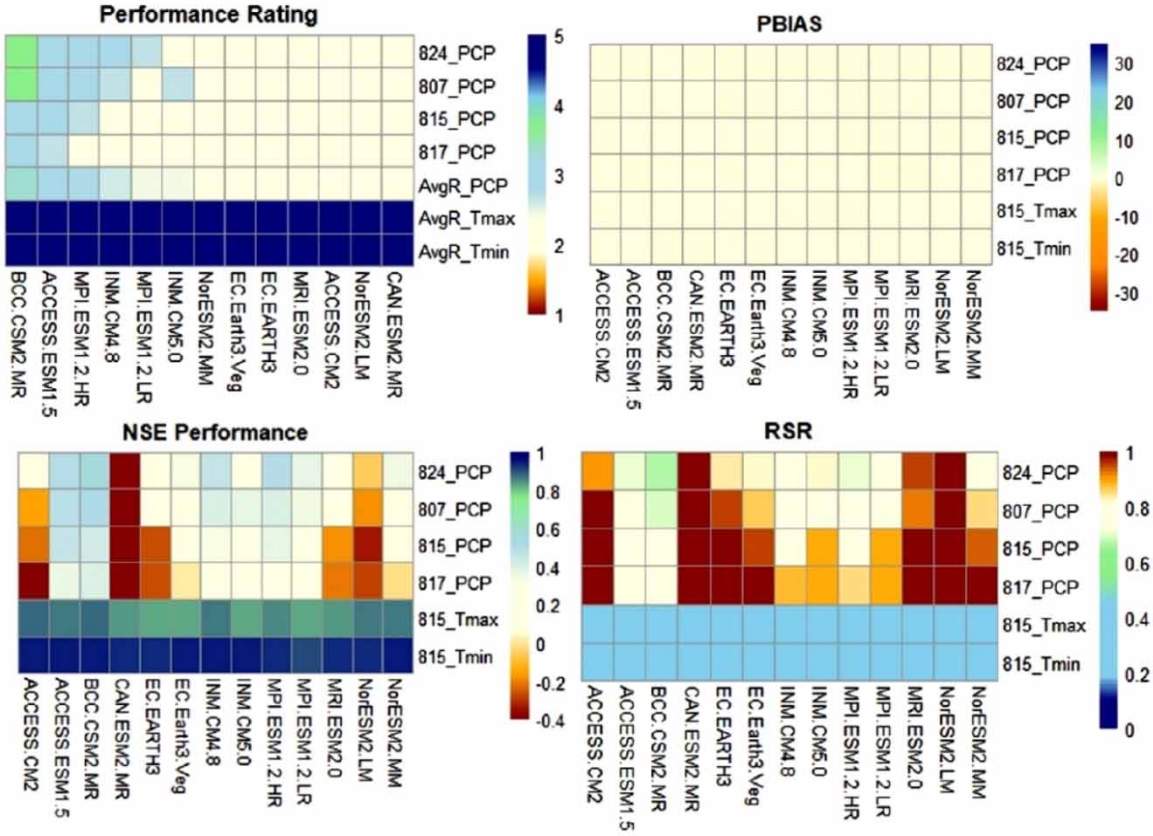

Figure 7 | Performance rating of BCMs. In the top-left sub-plot, ranking 1–13 follows the order while moving from left to right.

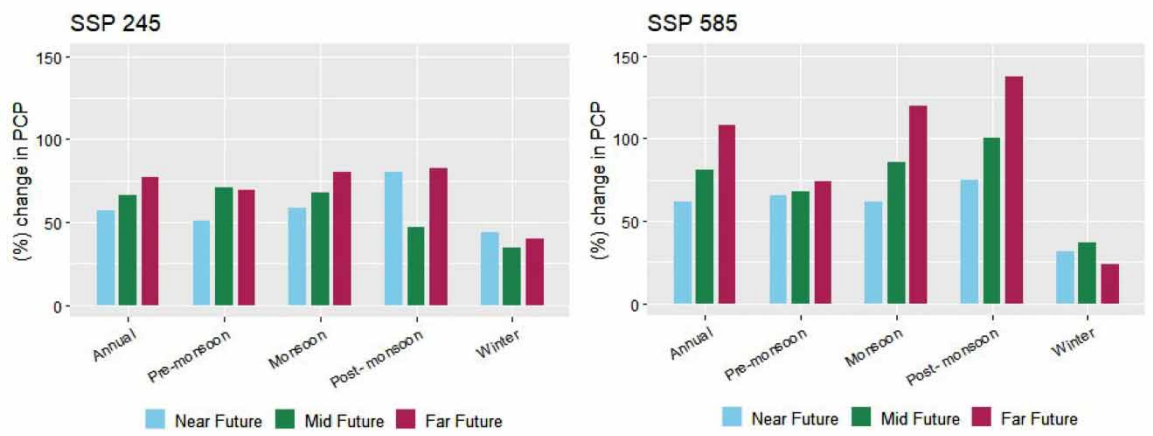

Figure 8 | Projected annual and seasonal change in precipitation for the Madi River Basin for near, mid, and far future under two socioeconomic pathways.

rains, such as dam overflow, increased sediment load, and potential structural failures. Addressing these challenges requires the incorporation of adaptive management strategies in the design and operation of hydropower systems, including enhanced spillway capacity, sediment management practices, integration of Integrated Water Resources Management (IWRM) approaches, and implementation of advanced forecasting and early warning systems to anticipate extreme weather events with reservoir operation protocols.

3.4.2. Projected temperature

The model representing the warmer climate is ACCESS-ESM1-5, while MPI-ESM1-2-LR and BCC-CSM2-MR exhibit characteristics of a colder climate. The average annual temperature from BCM, explored in Supplementary

Figure S2, reveals a pattern that is relatively consistent without drastic dips. Although there might be slight decreases or plateaus in certain years, the overall trajectory is an increment in temperature. With the historical baseline temperature at 23.42 °C, the increment in the FF period is approximately 1.8 °C for SSP245 and 3.5 °C for SSP585. Figure 9 (Supplementary Table S4) illustrates the percentage change in average annual and seasonal temperature. In the annual perspective, both scenarios indicate a progressive increase in temperature, with the SSP585 scenario showing a slightly more pronounced change, reaching 14.88% in the FF compared to 7.90% under SSP245. In seasonal breakdown, pre-monsoon temperatures are projected to rise in both scenarios, with the highest increase observed in SSP585-FF at 22.50%. During the monsoon and post-monsoon seasons, the percentage increase is relatively consistent across the two scenarios, although at different rates, ranging from 2.67 to 11.09% for monsoon and 2.75 to 12.88% for post-monsoon. Winter exhibits the most pronounced temperature changes, particularly in the SSP585 scenario, where the increase reaches up to 29.25% in the FF, in contrast to the baseline winter temperature of 16.47 °C. This warming may cause reduced winter streamflow, possibly due to increased evaporation or alterations in snow and ice melt patterns. Such fluctuations signal significant alterations in seasonal temperature dynamics that may entail broader climatic implications.

3.4.3. Projected streamflow

Supplementary Figure S3 illustrates the average annual flow along with the minimum and maximum flow projections from the climate models for both the SSP245 and SSP585 scenarios. Fluctuations are observed in the mean flow, with a range of 72.32–140.223 m^3/s for SSP245, and a slightly broader span of 73.13–192.78 m^3/s for SSP585. This contrasts with the historical baseline flow of 69.58 m^3/s, suggesting an overall increasing trend in the mean flow projection for both scenarios. The simulated annual variation in flow sets the stage for further examination of underlying impacts on monthly and seasonal flow patterns. The mean monthly hydrograph illustrated in Figure 10 offers a more detailed view of the streamflow trends. Both scenarios, SSP245 and SSP585, demonstrate slight flow reduction in January and increment in all other months with marked peak flows during monsoon season (June to August), reflecting the typical South Asian monsoon pattern. Particularly in the FF scenarios, SSP585 consistently forecasts higher flow values, such as 345 m^3/s, in contrast to 284 m^3/s for SSP245.

Expanding upon these insights, Figure 11 (Supplementary Table S5) details the average annual and seasonal changes in streamflow. These illustrate an increase in streamflow percentage changes across the annual, and all seasons in both SSP245 and SSP585 scenarios from NF to FF. Under SSP245, the annual streamflow change exhibits a steady increase from 34.07% in NF to 55.26% in FF. Seasonal variances are most pronounced in the monsoon, peaking at 62.27% in FF, and least in the winter, at 16.82% in FF. Conversely, SSP585 illustrates more dramatic fluctuations, with annual changes escalating from 38.71% in NF to an alarming 89.13% in FF. Seasonal spikes are most severe in the monsoon season, rising to 101.99% in FF, while the winter season experiences a comparatively subdued change of 13.65% in FF.

These collective changes in hydroclimatic variables present both challenges and opportunities for the Madi River Basin. The anticipated increases in precipitation and streamflow may enhance water resources and

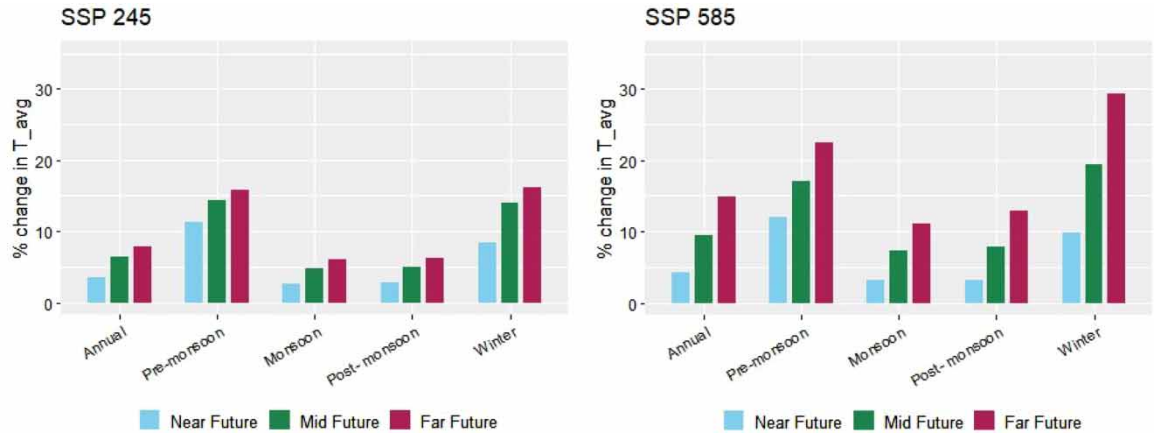

Figure 9 | Projected annual and seasonal change in temperature for the Madi River Basin for near, mid, and far future under two socioeconomic pathways.

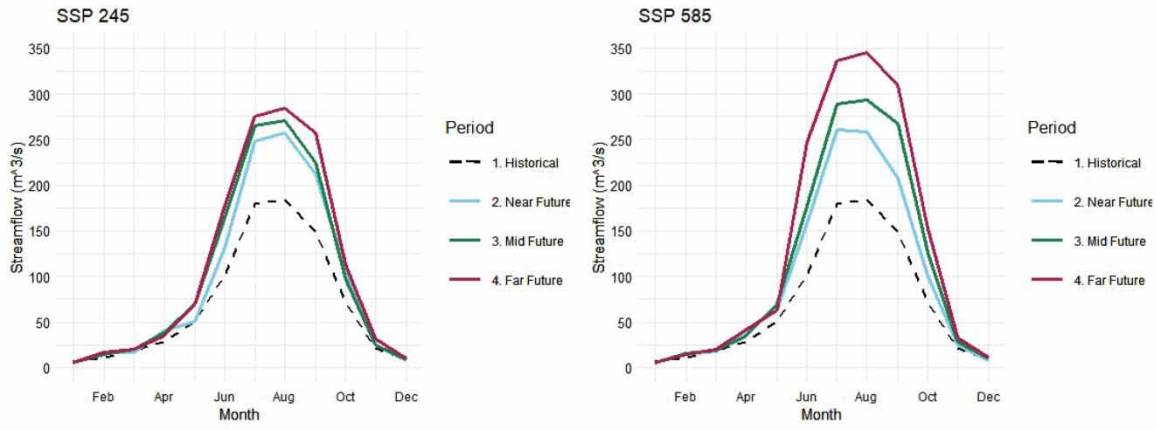

Figure 10 | Projected mean monthly hydrograph at the outlet for the Madi River Basin for near, mid, and far future under two socioeconomic pathways.

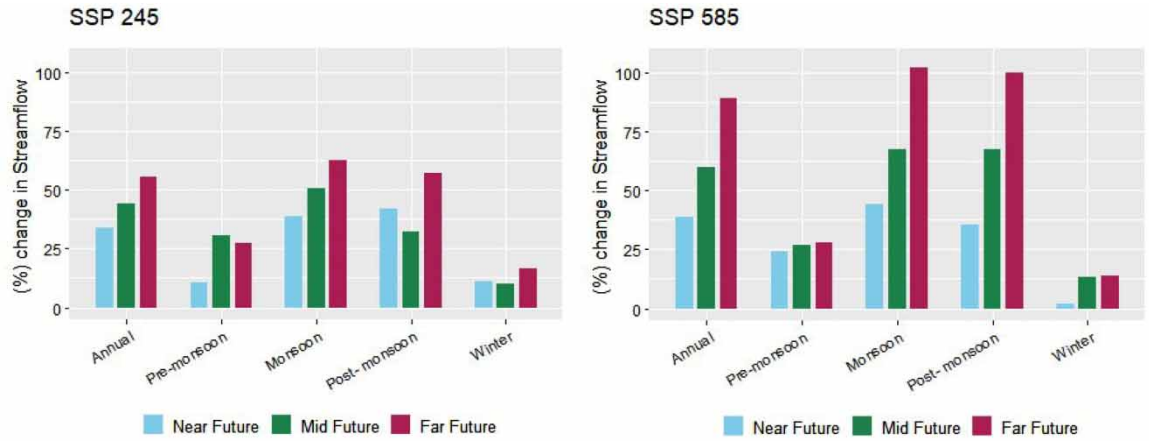

Figure 11 | Projected annual and seasonal change in streamflow at the outlet for the Madi River Basin for near, mid, and far future under two socioeconomic pathways.

energy generation but higher flow velocities can result in scouring, erosion, landslides, and increased pressure on dam structures, necessitating the implementation of robust design and maintenance standards, particularly during monsoon season. Such conditions not only pose a risk to the structural integrity of hydropower dams but also to the efficiency of energy production. Moreover, the integration of flexible operation strategies, such as adjustable turbine technology and modular dam designs, could enhance the resilience and adaptability of hydropower systems to fluctuating hydrological conditions. Additionally, diversifying the energy mix with renewable resources and strengthening policy and regulatory frameworks will ensure the longevity and reliability of hydropower projects. In conclusion, the streamflow data at the outlet of Madi River Basin shed light on the complex interplay of climatic and hydrological factors that govern the watershed's flow regime.

3.5. Implications for hydropower generation

Building upon the comprehensive analysis of streamflow and climate scenarios, this section explores three selected hydropower projects. The baseline energy is obtained from SWAT-simulated flow under the design specification of the respective hydropower projects. The projected fluctuations in energy generation from 2026 to 2100 are compared and analyzed with baseline energy, thereby interpreting their implications for the regional hydropower sector.

3.5.1. Energy generation from Super Madi HPP (44 MW)

Energy generation projections from six BCMs along with their mean values under two scenarios are shown in Figure 12. The baseline annual energy for the Super Madi project is 241.66 GWh. For both scenarios, there

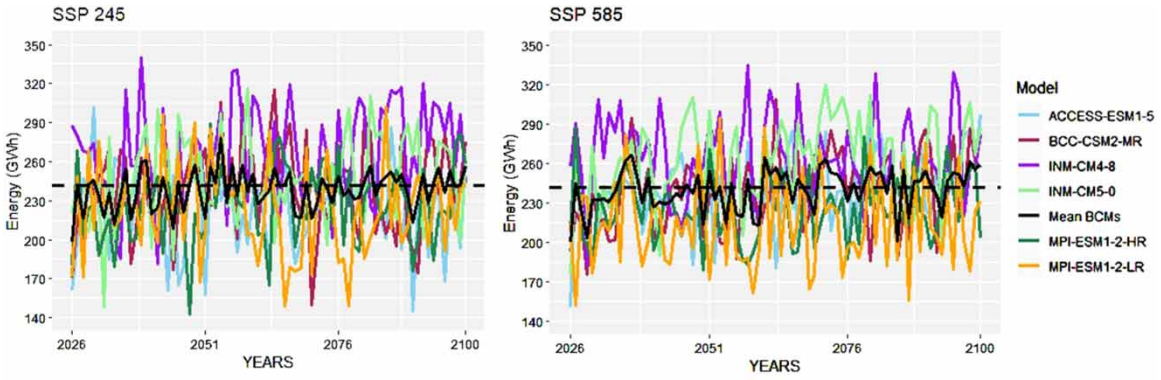

Figure 12 | Projected annual energy generation for Super Madi HPP using six BCM outputs for near, mid, and far future under two socioeconomic pathways.

are notable inter-annual fluctuations across the different models with gradually increasing directional trends over the years. The overall trend, represented by the mean values of the six models, exhibits frequent short-term increases in energy that surpass the baseline production in certain years for SSP245 and in most of the years for SSP585, indicating periods of potentially higher-than-expected renewable energy availability. Figure 13 represents the percentage relative monthly change under two scenarios. In both scenarios, the Super Madi HPP operates at full capacity during the monsoon months of July, August, and September, maintaining operational efficiency in all projected periods. Both SSP245 and SSP585 exhibited a substantial increment in February, particularly in the NF, with SSP245 reflecting a more pronounced increase, reaching 44.72%. Conversely, the maximum decrement is observed in January for both scenarios in all periods. Both scenarios exhibit similar trends and seasonal patterns, i.e., negative values in the first month, followed by positive or zero values from March to September and more negative values during October, November, and December.

A collective study of the annual and seasonal scale changes is depicted in Supplementary Table S6. In both scenarios, annual energy generation fluctuates modestly. Seasonally, the pre-monsoon and winter periods manifest the most considerable increment in SSP245 with pre-monsoon rising to 13.90% in MF and winter to 8.13% in the FF. In SSP585, pre-monsoon witnessed the most substantial rise, reaching up to 15.06% in FF, while winter and post-monsoon seasons demonstrated more tempered adjustments.

3.5.2. Energy generation from Madame Khola HPP (24 MW)

Figure 14 represents the energy generation projections from six BCMs, along with their mean values, under two scenarios. The baseline annual energy for the Madame Khola project is 135.8 GWh. In both scenarios, the fluctuations between the models signify an inherent uncertainty and complexity in the projection. The mean values

Figure 13 | Projected monthly change in energy generation for Super Madi HPP for near, mid, and far future under two socioeconomic pathways.

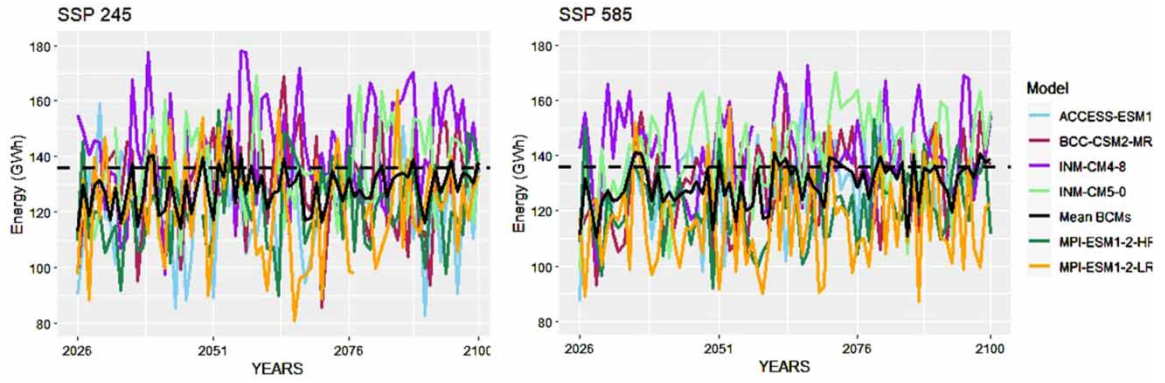

Figure 14 | Projected annual energy generation for Madame Khola HPP using six BCM outputs for near, mid, and far future under two socioeconomic pathways.

reflect a very gradual and irregular increase in energy generation, where only a few years are projected to generate energy equal to or marginally surpassing the baseline. Contrary to the trends observed in the Super Madi Project, this observation emphasizes a careful balance between growth and fluctuation, suggesting underlying patterns that may be due to broader climatic or methodological factors. Figure 15 elucidates the percentage relative monthly change under two scenarios. In alignment with the Super Madi HPP, this hydropower project also maintains full operational efficiency during the monsoon season, encompassing July, August, and September. Under the SSP245 scenario, a notable rise in energy generation of 39.49% is observed in February of the NF, while a substantial decline of −44.07% manifests in January of the FF. In contrast, the SSP585 scenario portrays a distinct decrement in January across all timeframes, plunging to as low as −41.36% in the FF, but demonstrates a remarkable increment of 33% in December of the MF. Both scenarios exhibit a similar seasonal pattern: initial negative percentages in January are followed by either zero or positive values from March through September and negative or positive fluctuations thereafter.

Furthermore, an examination of the annual and seasonal fluctuations in energy generation is portrayed in Supplementary Table S7. Under the SSP245 scenario, modest annual changes are accompanied by noteworthy seasonal increments; the pre-monsoon and winter seasons exhibit the most significant rises, peaking at 12.05 and 11.72% in the NF, respectively. Similarly, the SSP585 scenario manifests modest annual shifts but presents pronounced seasonal variations. The pre-monsoon season experiences the most substantial increment, reaching 7.30% in the FF, while the winter season demonstrates a divergent trend, declining to −5.38% in the FF. These variations under both scenarios underscore the differentiated impacts of climatic alterations on energy generation across annual and seasonal timescales.

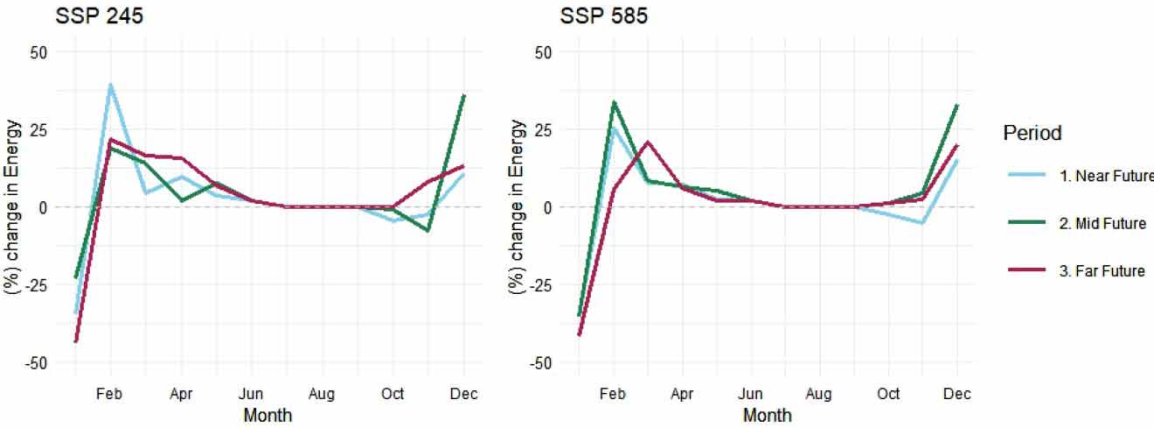

Figure 15 | Projected monthly change in energy generation for Madame Khola HPP for near, mid, and far future under two socioeconomic pathways.

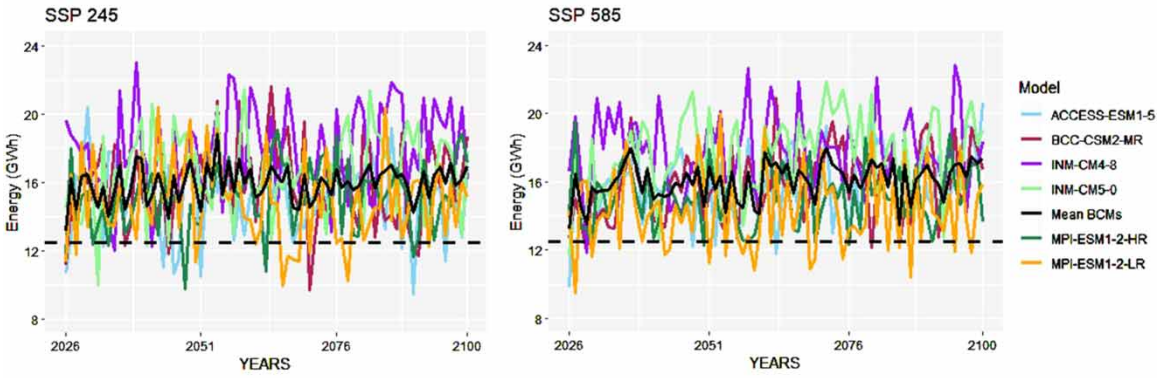

Figure 16 | Projected annual energy generation for Midim Khola HPP using six BCM outputs for near, mid, and far future under two socioeconomic pathways.

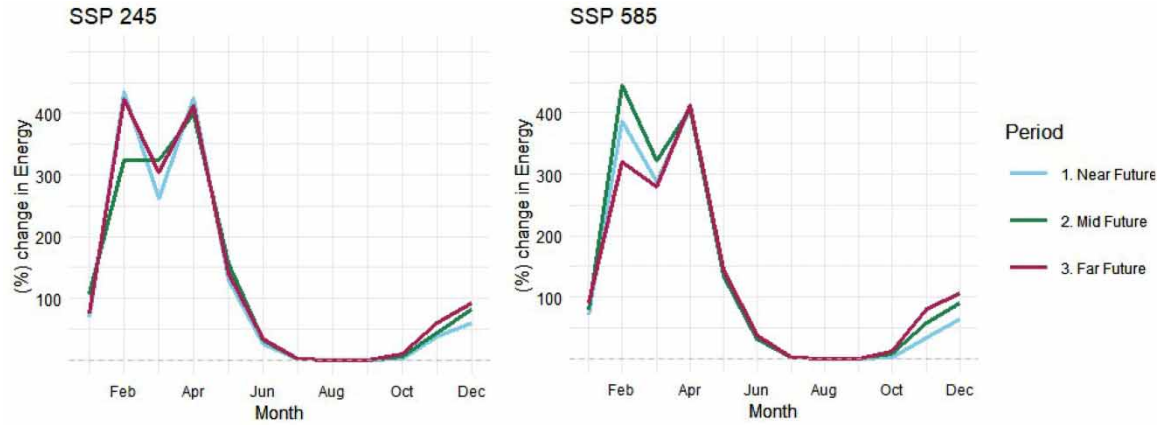

Figure 17 | Projected monthly change in energy generation for Midim Khola HPP for near, mid, and far future under two socioeconomic pathways.

3.5.3. Energy generation from Midim Khola HPP (3 MW)

Figure 16 delineates the annual energy generation from six BCMs under two distinct scenarios. Contrary to previous projects, the projection for the Midim Khola project is characterized by consistent and incremental growth in energy generation that constantly surpasses the baseline levels of 12.5 GWh. This trend is indicative of a promising future in energy production. However, it is worth noting that there is a marked inter-model variability in all projections. Overall, the project demonstrates resilience and adaptability in its potential energy generation for the future, despite the fluctuations and complexities in modeling. Figure 17 illustrates the monthly relative change for the project under two scenarios. The data signify pronounced increments in the early months, specifically from February to April, where changes surpass threefold in almost all periods for both scenarios. This trend is anticipated to persist in the late months, from October to December, with significant increments evident. Conversely, the monsoon months except July observe a slight decrement, which may give rise to operational inconsistencies.

A summative analysis of the annual and seasonal variations in energy generation is presented in Supplementary Table S8. Under the SSP245 scenario, there is a remarkable surge in annual energy generation, peaking at 29.27% in the FF. The most significant seasonal increment is observed in the pre-monsoon period, reaching 231.06% in FF. In contrast, the SSP585 scenario shows its maximum annual change at 40.28% in the MF, with the pre-monsoon season also witnessing the most significant rise at 356.46%. In both scenarios, the winter season demonstrates relatively modest increases, reaching up to 194.02% in SSP585 during the MF.

4. CONCLUSIONS

To bridge the existing knowledge gap regarding the critical implications of climate change on Nepal's hydropower sector, we designed a study focused on the Madi River Basin. The methodologies and insights derived

from this study can be applied to other basins with similar characteristics, thus extending the relevance of the findings to a broader hydroclimatic context. In summary, this study affirms the robustness of the SWAT model for hydrological assessments in the Madi River Basin, achieving 'Very Good' performance (both R^2 and NSE greater than 0.8). The necessity for bias correction in CMIP6 GCMs was highlighted, particularly for precipitation variables. Application of the linear scaling method markedly enhanced the predictive reliability, with BCC-CSM2-MR emerging as the better-performing model. Six models were chosen for future climate projection, underscoring the importance of correction in reliable climate impact assessments. Projected analysis reveals an increase in annual precipitation by 76.64% under SSP245 and 108.24% under SSP585 in the far future when compared with the historical baseline level of 2,240.13 mm. Concurrently, the temperature is predicted to follow a consistent upward trajectory, leading to increments of 1.8 and 3.5 °C in the far future under differing scenarios. Increments in annual mean flow fluctuations, ranging from 72.32 to 192.78 m^3/s under differing scenarios, from a historical baseline flow of 69.58 m^3/s. To enhance the resilience of hydropower systems against the challenges posed by climate change-induced extreme hydrological events, it is crucial to adopt adaptive management strategies, including the implementation of enhanced spillway capacities and advanced forecasting and early warning systems, alongside the integration of robust design standards to mitigate risks from increased sediment load, dam overflow, and structural pressures due to high rains and increased flow velocities.

This study also emphasizes the heterogeneous nature of hydropower potential across different projects within the basin. For instance, Super Madi HPP represents hydropower projects within the main river. Here, annual energy generation is projected to increase by 4.88% under SSP245 and 4.95% under SSP585 in the far future timeframe. Similarly, Madame Khola HPP illustrates the unique challenges faced by projects in the upper tributaries and upper elevations. For the Madame project, annual energy generation in the far future is projected to increase by 3.83 and 2.06% under SSP245 and SSP585, respectively. Both projects are characterized by gradual increases in energy generation, and seasonal patterns of full-capacity operation during monsoon months emphasizing the project's adaptability to varying climatic conditions. Furthermore, Midim Khola HPP presents an encouraging picture for small-scale projects in lower tributaries and middle-lower elevations with annual increment in the far future by 29.27% under SSP245 and 30.6% under SSP585 demonstrating consistent and incremental growth in energy generation. Such outcomes underscore the necessity for location-specific planning and strategic management in optimizing renewable energy sources. The Madi River Basin's projected increase in streamflow and precipitation does not uniformly translate into a corresponding trend in hydropower generation across different projects, revealing the intricate interplay between hydrological variables, hydraulic constraints, and energy production. These results can offer valuable insights for facilitating the planning and development of sustainable energy management and climate adaptation strategies, in evolving global climate challenges.

ACKNOWLEDGEMENTS

The authors would like to express sincere thanks to Er. Rupesh Baniya from Nepal Development Research Institute, for his support and invaluable advice during the study, which were instrumental to the success of this study.

DATA AVAILABILITY STATEMENT

All relevant data are included in the paper or its Supplementary Information.

CONFLICT OF INTEREST

The authors declare there is no conflict.

REFERENCES

Abbaspour, K. C., Rouholahnejad, E., Vaghefi, S., Srinivasan, R., Yang, H. & Kløve, B. 2015 A continental-scale hydrology and water quality model for Europe: Calibration and uncertainty of a high-resolution large-scale SWAT model. *Journal of Hydrology* **524**, 733–752. https://doi.org/10.1016/j.jhydrol.2015.03.027.

Abbaspour, K., Vaghefi, S. & Srinivasan, R. 2017 A guideline for successful calibration and uncertainty analysis for soil and water assessment: A review of papers from the 2016 international SWAT conference. *Water* **10** (1), 6. https://doi.org/10.3390/w10010006.

Allen, R. G., Pereira, L. S., Raes, D. & Smith, M. 1998 Crop Evapotranspiration – Guidelines for Computing Crop Water Requirements – FAO Irrigation and Drainage Paper 56. FAO, Rome, 300(9): D05109.

Arnold, J. G., Srinivasan, R., Muttiah, R. S. & Williams, J. R. 1998 Large area hydrologic modeling and assessment part I: Model development. *Journal of the American Water Resources Association* **34** (1), 73–89. https://doi.org/10.1111/j.1752-1688.1998.tb05961.x.

Arnold, J. G., Moriasi, D. N., Gassman, P. W., Abbaspour, K. C., White, M. J., Srinivasan, R., Santhi, C., Harmel, R. D., van Griensven, A., Van Liew, M. W., Kannan, N. & Jha, M. K. 2012 SWAT: Model use, calibration, and validation. *Transactions of the ASABE* **55** (4), 1491–1508. https://doi.org/10.13031/2013.42256.

Babel, M. S., Bhusal, S. P., Wahid, S. M. & Agarwal, A. 2014 Climate change and water resources in the Bagmati River Basin, Nepal. *Theoretical and Applied Climatology* **115** (3–4), 639–654. https://doi.org/10.1007/s00704-013-0910-4.

Bajracharya, S. R. & Shrestha, B. R. 2011 The status of glaciers in the Hindu Kush-Himalayan region. In: *International Centre for Integrated Mountain Development (ICIMOD)*.

Baniya, R. 2022 *Integrated Modeling for Assessing Climate Change Impact and Uncertainty on Hydropower Potential in the Central Himalayas: A Case Study of Tila River Basin*. Master's Thesis, Institute of Engineering, Tribhuvan University.

Baniya, R., Talchabhadel, R., Panthi, J., Ghimire, G. R., Sharma, S., Khadka, P. D., Shin, S., Pokhrel, Y., Bhattarai, U., Prajapati, R. & Thapa, B. R. 2023 Nepal Himalaya offers considerable potential for pumped storage hydropower. *Sustainable Energy Technologies and Assessments* **60**, 103423. https://doi.org/10.1016/j.seta.2023.103423.

Barzkar, A., Najafzadeh, M. & Homaei, F. 2022 Evaluation of drought events in various climatic conditions using data-driven models and a reliability-based probabilistic model. *Natural Hazards* **110** (3), 1931–1952. https://doi.org/10.1007/s11069-021-05019-7.

Bhattarai, R., Aryal, D., Timilsina, A. & Yadav, S. 2016 Hydrological modeling under climate change scenarios: A case study of the Koshi River Basin, Nepal. *Water* **8** (4), 138.

Bhattarai, S. N., Zhou, Y., Shakya, N. M. & Zhao, C. 2018 Hydrological modelling and climate change impact assessment using HBV light model: A case study of Narayani River Basin. *Nature Environment and Pollution Technology* **17** (3), 691–702.

Bista, S., Singh, U., Kayastha, N., Ghimire, B. N. & Talchabhadel, R. 2021 Effects of source digital elevation models in assessment of gross run-off-river hydropower potential: A case study of West Rapti Basin Nepal. *Journal of Engineering Issues and Solutions* **1** (1), 106–128.

Burgan, H. I. 2022 Comparison of different ANN (FFBP, GRNN, RBF) algorithms and multiple linear regression for daily streamflow prediction in Kocasu River, Turkey. *Fresenius Environment Bulletin* **31**, 4699–4708.

Chhetri, R., Pandey, V. P., Talchabhadel, R. & Thapa, B. R. 2021 How do CMIP6 models project changes in precipitation extremes over seasons and locations across the mid hills of Nepal? *Theoretical and Applied Climatology* **145** (3–4), 1127–1144. https://doi.org/10.1007/s00704-021-03698-7.

Dahal, P., Shrestha, N. S., Shrestha, M. L., Krakauer, N. Y., Panthi, J., Pradhanang, S. M., Jha, A. & Lakhankar, T. 2016a Drought risk assessment in central Nepal: Temporal and spatial analysis. *Natural Hazards* **80** (3), 1913–1932. https://doi.org/10.1007/s11069-015-2055-5.

Dahal, V., Shakya, N. M. & Bhattarai, R. 2016b Estimating the impact of climate change on water availability in Bagmati Basin, Nepal. *Environmental Processes* **3** (1), 1–17. https://doi.org/10.1007/s40710-016-0127-5.

Devkota, L. P. & Gyawali, D. R. 2015 Impacts of climate change on hydrological regime and water resources management of the Koshi River Basin, Nepal. *Journal of Hydrology: Regional Studies* **4**, 502–515. https://doi.org/10.1016/j.ejrh.2015.06.023.

Dhakal, S., Shakya, S. R. & Bajracharya, S. R. 2017 Hydropower in Nepal: Opportunities and challenges. *Renewable and Sustainable Energy Reviews* **81**, 1731–1737.

Dhakal, S., Srivastava, L., Sharma, B., Palit, D., Mainali, B., Nepal, R., Purohit, P., Goswami, A., Malikyar, G. M. & Wakhley, K. B. 2019 Meeting future energy needs in the Hindu Kush Himalaya. In: *The Hindu Kush Himalaya Assessment*. Springer International Publishing, pp. 167–207. https://doi.org/10.1007/978-3-319-92288-1_6.

Dijkshoorn, K. & Huting, J. 2009 Soil and Terrain database for Nepal. ISRIC – World Soil Information. Wageningen 29

Eyring, V., Bony, S., Meehl, G. A., Senior, C. A., Stevens, B., Stouffer, R. J. & Taylor, K. E. 2016 Overview of the Coupled Model Intercomparison Project Phase 6 (CMIP6) experimental design and organization. *Geoscientific Model Development* **9** (5), 1937–1958. https://doi.org/10.5194/gmd-9-1937-2016.

Forest Research and Training Centre (FRTC), & International Centre for Integrated Mountain Development (ICIMOD) 2021 *Land cover of Nepal* [Data set]. Ministry of Forests and Environment, Government of Nepal; ICIMOD. Updated on 2022-04-21. https://doi.org/10.26066/RDS.1972729

Gassman, P. W., Reyes, M. R., Green, C. H. & Arnold, J. G. 2007 The soil and water assessment tool: Historical development, applications, and future research directions. *Transactions of the ASABE* **50** (4), 1211–1250. https://doi.org/10.13031/2013.23637.

Greve, P., Gudmundsson, L. & Seneviratne, S. I. 2018 Regional scaling of annual mean precipitation and water availability with global temperature change. *Earth System Dynamics* **9** (1), 227–240. https://doi.org/10.5194/esd-9-227-2018.

Haddeland, I., Heinke, J., Biemans, H., Eisner, S., Flörke, M., Hanasaki, N., Konzmann, M., Ludwig, F., Masaki, Y., Schewe, J., Stacke, T., Tessler, Z. D., Wada, Y. & Wisser, D. 2014 Global water resources affected by human interventions and climate change. *Proceedings of the National Academy of Sciences* **111** (9), 3251–3256. https://doi.org/10.1073/pnas.1222475110.

Hamududu, B. & Killingtveit, A. 2012 Assessing climate change impacts on global hydropower. *Energies* **5** (2), 305–322. https://doi.org/10.3390/en5020305.

Hegerl, G. C., Black, E., Allan, R. P., Ingram, W. J., Polson, D., Trenberth, K. E., Chadwick, R. S., Arkin, P. A., Sarojini, B. B., Becker, A., Dai, A., Durack, P. J., Easterling, D., Fowler, H. J., Kendon, E. J., Huffman, G. J., Liu, C., Marsh, R., New, M. & Zhang, X. 2015 Challenges in quantifying changes in the global water cycle. *Bulletin of the American Meteorological Society* **96** (7), 1097–1115. https://doi.org/10.1175/BAMS-D-13-00212.1.

Huss, M. & Hock, R. 2018 Global-scale hydrological response to future glacier mass loss. *Nature Climate Change* **8** (2), 135–140.

IHA 2021 *Hydropower Status Report*. International Hydropower Association.

Immerzeel, W. W., Lutz, A. F., Andrade, M., Bahl, A., Biemans, H., Bolch, T., Hyde, S., Brumby, S., Davies, B. J., Elmore, A. C., Emmer, A., Feng, M., Fernández, A., Haritashya, U., Kargel, J. S., Koppes, M., Kraaijenbrink, P. D. A., Kulkarni, A. V., Mayewski, P. A. & Baillie, J. E. M. 2020 Importance and vulnerability of the world's water towers. *Nature* **577** (7790), 364–369. https://doi.org/10.1038/s41586-019-1822-y.

IPCC 2013 Summary for policymakers. In: *Climate Change 2013: The Physical Science Basis. Contribution of Working Group I to the Fifth Assessment Report of the Intergovernmental Panel on Climate Change* (Stocker, T. F., Qin, D., Plattner, G.-K., Tignor, M., Allen, S. K., Boschung, J., Nauels, A., Xia, Y., Bex, V. & Midgley, P. M., eds). Cambridge University Press, Cambridge, UK, and New York, NY, USA.

IPCC 2014 Climate Change 2014: Synthesis Report. Contribution of Working Groups I, II and III to the Fifth Assessment Report of the Intergovernmental Panel on Climate Change. Geneva, Switzerland.

IPCC 2018 *Global Warming of 1.5 °C. Special Report Intergovernmental Panel on Climate Change.*

IPCC 2019 Climate Change and Land: An IPCC Special Report on Climate Change, Desertification, Land Degradation, Sustainable Land Management, Food Security, and Greenhouse Gas Fluxes in Terrestrial Ecosystems [P.R. Shukla, J. Skea, E. Calvo Buendia, V. Masson-Delmotte, H.-O. Pörtner, D. C. Roberts, P. Zhai, R. Slade, S. Connors, R. van Diemen, M. Ferrat, E. Haughey, S. Luz, S. Neogi, M. Pathak, J. Petzold, J. Portugal Pereira, P. Vyas, E. Huntley, K. Kissick, M. Belkacemi, J. Malley (eds.)]

IRENA 2020 *Innovation Outlook: Renewable Mini-Grids*. International Renewable Energy Agency, Abu Dhabi.

Kandel, S., Khadka, N., Tiwari, D., Shrestha, D. & Rijal, K. 2023 Evolution and bathymetry of glacial lake at the lowest elevation in Nepal Himalaya. *Journal of Mountain Science* **20** (1), 141–144. https://doi.org/10.1007/s11629-022-7615-z.

Kendall, M. G. 1975 *Rank Correlation Methods*, 4th edn. Charles Griffin, London.

Khadka, D., Babel, M. S., Shrestha, S. & Tripathi, N. K. 2014 Climate change impact on glacier and snow melt and runoff in Tamakoshi basin in the Hindu Kush Himalayan (HKH) region. *Journal of Hydrology* **511**, 49–60. https://doi.org/10.1016/j.jhydrol.2014.01.005.

Khanal, N. & Watanabe, T. 2017 Low-flow hydrology in the Nepal Himalaya. *Geographical Studies* **92** (1), 6–16. https://doi.org/10.7886/hgs.92.6.

Koirala, R., Thapa, B., Neopane, H. P., Zhu, B. & Chhetry, B. 2016 Sediment erosion in guide vanes of Francis turbine: A case study of Kaligandaki Hydropower Plant, Nepal. *Wear* **362–363**, 53–60. https://doi.org/10.1016/j.wear.2016.05.013.

Koirala, S., Oglethorpe, J., Khanal, K., Dhakal, S., Poudel, K. R., Sharma, K. & Bhandari, K. 2017 Temporal change detection of Kahphuche glacial lake Kaski District, Nepal. *Journal of Nepal Geological Society* **53**, 119–122.

Krause, P., Boyle, D. P. & Bäse, F. 2005 Comparison of different efficiency criteria for hydrological model assessment. *Advances in Geosciences* **5**, 89–97. https://doi.org/10.5194/adgeo-5-89-2005.

Lamsal, G. R., Basnyat, D. B., Kafle, M. R. & Baniya, R. 2023 Optimal operation of cascading reservoirs in Koshi river basin. *International Journal of Energy and Water Resources* 1–12. https://doi.org/10.1007/s42108-023-00243-2.

Madani, K. & Lund, J. R. 2010 Estimated impacts of climate warming on California's high-elevation hydropower. *Climatic Change* **102** (3–4), 521–538. https://doi.org/10.1007/s10584-009-9750-8.

Mann, H. B. 1945 Nonparametric tests against trend. *Econometrica* **13** (3), 245. https://doi.org/10.2307/1907187.

Maraun, D., Wetterhall, F., Ireson, A. M., Chandler, R. E., Kendon, E. J., Widmann, M., Brienen, S., Rust, H. W., Sauter, T., Themeßl, M., Venema, V. K. C., Chun, K. P., Goodess, C. M., Jones, R. G., Onof, C., Vrac, M. & Thiele-Eich, I. 2010 Precipitation downscaling under climate change: Recent developments to bridge the gap between dynamical models and the end user. *Reviews of Geophysics* **48** (3), RG3003.1–RG3003.29.

Milly, P. C. D., Betancourt, J., Falkenmark, M., Hirsch, R. M., Kundzewicz, Z. W., Lettenmaier, D. P. & Stouffer, R. J. 2008 Stationarity is dead: Whither water management? *Science* **319** (5863), 573–574. https://doi.org/10.1126/science.1151915.

Mishra, V., Bhatia, U. & Tiwari, A. D. 2020 Bias-corrected climate projections for South Asia from coupled model intercomparison project-6. *Scientific Data* **7** (1), 338. https://doi.org/10.1038/s41597-020-00681-1.

Moriasi, D. N., Arnold, J. G., Van Liew, M. W., Bingner, R. L., Harmel, R. D. & Veith, T. L. 2007 Model evaluation guidelines for systematic quantification of accuracy in watershed simulations. *Transactions of the ASABE* **50** (3), 885–900. https://doi.org/10.13031/2013.23153.

NDC 2020 *Nepal's Nationally Determined Contributions*. Government of Nepal, Kathmandu.

NEA 2022 *Annual Report*. Nepal Electricity Authority.

Neitsch, S. L., Arnold, J. G., Kiniry, J. R. & Williams, J. R. 2011 *Soil and Water Assessment Tool: Theoretical Documentation Version 2009*. Texas Water Resources Institute, College Station, TX.

Ojha, H., Neupane, K. R., Pandey, C. L., Singh, V., Bajracharya, R. & Dahal, N. 2020 Scarcity amidst plenty: Lower Himalayan cities struggling for water security. *Water* **12** (2), 567. https://doi.org/10.3390/w12020567.

O'Neill, B. C., Tebaldi, C., van Vuuren, D. P., Eyring, V., Friedlingstein, P., Hurtt, G., Knutti, R., Kriegler, E., Lamarque, J.-F., Lowe, J., Meehl, G. A., Moss, R., Riahi, K. & Sanderson, B. M. 2016 The scenario model intercomparison project (ScenarioMIP) for CMIP6. *Geoscientific Model Development* **9** (9), 3461–3482. https://doi.org/10.5194/gmd-9-3461-2016.

Pandey, V. P., Shrestha, S. & Kazama, F. 2018 Assessment of climate change impact on floods from a model comparison exercise. *Scientific Reports* **8** (1), 3843.

Pandey, V. P., Dhaubanjar, S., Bharati, L. & Thapa, B. R. 2020 Spatio-temporal distribution of water availability in Karnali-Mohana Basin, Western Nepal: Hydrological model development using multi-site calibration approach (Part-A). *Journal of Hydrology: Regional Studies* **29**, 100690. https://doi.org/10.1016/j.ejrh.2020.100690.

Pokharel, N., Basnet, K., Sherchan, B. & Thapaliya, D. 2020 *Assessment of Hydropower Potential Using SWAT Modeling and Spatial Technology in the Seti Gandaki River*. IEEE-SEM, Kaski, Nepal. ISSN 2320-9151.

Poudel, D. D. & Duex, T. W. 2017 Vanishing springs in Nepalese mountains: Assessment of water sources, farmers' perceptions, and climate change adaptation. *Mountain Research and Development* **37** (1), 35. https://doi.org/10.1659/MRD-JOURNAL-D-16-00039.1.

Ragettli, S., Pellicciotti, F., Immerzeel, W. W., Miles, E. S., Petersen, L., Heynen, M., Shea, J. M., Stumm, D., Joshi, S. & Shrestha, A. 2015 Unraveling the hydrology of a Himalayan catchment through integration of high resolution in situ data and remote sensing with an advanced simulation model. *Advances in Water Resources* **78**, 94–111. https://doi.org/10.1016/j.advwatres.2015.01.013.

Regmi, B. R., Star, C. & Leal Filho, W. 2016 Effectiveness of the local adaptation plan of action to support climate change adaptation in Nepal. *Mitigation and Adaptation Strategies for Global Change* **21** (3), 461–478. https://doi.org/10.1007/s11027-014-9610-3.

Reidmiller, D., Hayhoe, K., Easterling, D. R., Fahey, D. W., Doherty, S. J., Kossin, J., Sweet, W., Vose, R. S., Wehner, M. F., Wuebbles, D. J., Kopp, R. E., Kunkel, K. & Nielsen-Gammon, J. W. 2018 Climate science in the fourth US national climate assessment. In: *AGU Fall Meeting Abstracts*, Vol. 2018, Washington, DC, 10-14 December 2018. AGU, Washington, DC, pp. U24A-01.

Riahi, K., van Vuuren, D. P., Kriegler, E., Edmonds, J., O'Neill, B. C., Fujimori, S., Bauer, N., Calvin, K., Dellink, R., Fricko, O., Lutz, W., Popp, A., Cuaresma, J. C., K, S, . Leimbach, C., Jiang, M., Kram, L., Rao, T., Emmerling, S. & Tavoni, J. M. 2017 The shared socioeconomic pathways and their energy, land use, and greenhouse gas emissions implications: An overview. *Global Environmental Change* **42**, 153–168. https://doi.org/10.1016/j.gloenvcha.2016.05.009.

Sen, P. K. 1968 Estimates of the regression coefficient based on Kendall's Tau. *Journal of the American Statistical Association* **63** (324), 1379–1389. https://doi.org/10.1080/01621459.1968.10480934.

Shrestha, U. B., Gautam, S. & Bawa, K. S. 2012 Widespread climate change in the Himalayas and associated changes in local ecosystems. *PLoS ONE* **7** (5), e36741.

Shrestha, A. B., Aryal, S., Shrestha, U. B., Cho, Y. D., Shrestha, R. B., Shrestha, B. B. & Sharma, R. 2013 Modelling climate change implications on water resources in the Gandaki River Basin, Nepal. *International Journal of Water Resources Development* **29** (2), 132–151.

Shrestha, M., Acharya, S. C. & Shrestha, P. K. 2017 Bias correction of climate models for hydrological modelling – are simple methods still useful? *Meteorological Applications* **24** (3), 531–539. https://doi.org/10.1002/met.1655.

Shrestha, A., Aryal, S., Shrestha, U. B., Cho, Y. D., Shrestha, R. B., Shrestha, B. B. & Sharma, R. 2019 Climate change impact assessment and adaptation strategies for agriculture in the Gandaki River Basin, Nepal. *Atmosphere* **10** (12), 774.

Teutschbein, C. & Seibert, J. 2012 Bias correction of regional climate model simulations for hydrological climate-change impact studies: Review and evaluation of different methods. *Journal of Hydrology* **456–457**, 12–29. https://doi.org/10.1016/j.jhydrol.2012.05.052.

Timilsina, A., Talchabhadel, R. & Pandey, V. P. 2021 Rising temperature trends across the Narayani river Basin in Central Nepal projected by CMIP6 models. In: *Proceedings of 10th IOE Graduate Conference. Institute of Engineering, Tribhuvan University, Nepal*, pp. 266–278.

UNFCCC 2015 Adoption of the Paris Agreement. United Nations Framework Convention on Climate Change.

Van Lanen, H. A. J., Laaha, G., Kingston, D. G., Gauster, T., Ionita, M., Vidal, J., Vlnas, R., Tallaksen, L. M., Stahl, K., Hannaford, J., Delus, C., Fendekova, M., Mediero, L., Prudhomme, C., Rets, E., Romanowicz, R. J., Gailliez, S., Wong, W. K., Adler, M., Blauhut, V., Caillouet, L., Chelcea, S., Frolova, N., Gudmundsson, L., Hanel, M., Haslinger, K., Kohn, I., Lloyd-Hughes, B., Maskey, S., Mathbout, S., Melsen, L. A., Mishra, V., Pechlivanidis, I. G., Querner, E. P., Seneviratne, S. I. & Van Loon, A. F. 2016 Hydrology needed to manage droughts: The 2015 European case. *Hydrological Processes* **30** (17), 3097–3104. https://doi.org/10.1002/hyp.10838.

van Vliet, M. T. H., Franssen, W. H. P., Yearsley, J. R., Ludwig, F., Haddeland, I., Lettenmaier, D. P. & Kabat, P. 2013 Global river discharge and water temperature under climate change. *Global Environmental Change* **23** (2), 450–464. https://doi.org/10.1016/j.gloenvcha.2012.11.002.

WECS 2019 *Water Resources of Nepal in the Context of Climate Change*. Water and Energy Commission Secretariat, Government of Nepal, Kathmandu.

WECS 2022 *National Water Plan – Nepal*. Water and Energy Commission Secretariat, Government of Nepal, Kathmandu.

Xu, J., Grumbine, R. E., Shrestha, A., Eriksson, M., Yang, X., Wang, Y. & Wilkes, A. 2009 The melting Himalayas: Cascading effects of climate change on water, biodiversity, and livelihoods. *Conservation Biology* **23** (3), 520–530. https://doi.org/10.1111/j.1523-1739.2009.01237.x.

Zhang, X., Srinivasan, R., Zhao, K. & Liew, M. V. 2009 Evaluation of global optimization algorithms for parameter calibration of a computationally intensive hydrologic model. *Hydrological Processes* **23** (3), 430–441. https://doi.org/10.1002/hyp.7152.

First received 3 December 2023; accepted in revised form 28 February 2024. Available online 9 March 2024